

Republic of Iraq
Ministry of Higher Education
and Scientific Research
Al-Nahrain University
College of Science
Department of Physics



Preparation of Novel High Temperature Superconductor Compounds (Cu-1223 and Sn-1223) From Hg-1223

A thesis

submitted to college of Science / Al-Nahrain University as
a partial fulfillment of the requirements for the degree of
Master of Science in Physics

By

Israa Maher Jamal Taher

B.sc.Physics /College of Science / Al-Nahrain University

Supervised by

Prof. Dr. Emad Khudair Al-Shakarchi

July, 2017

Tho Alquda, 1438

الأهداء

إلى أبي الذي رسمني وأمي التي لوتني

وزوجي الذي احبني وساندني .

Acknowledgment

Firstly, I would like to thank God for helping me to make my dream a true by accomplishing thesis. This would not have happened without the efforts of my supervisor Prof. Emad Al-Shakarchi who directed me in each details. Then, I would like to thank my supportive husband Ahmed all the time and he would be forever, hopefully. Thanks for my lovely daughter who enhance me to complete my thesis. My gratitude to my parents for their encouragement all these years. I would like to thank my parents in law who had done the same role and support as my real parents. I appreciate their parental emotions. I would like to thank Dr.Stefano Loreti/ENEA Recherche Center / Italy for accessing the program (XRD) qualitative analysis. Again, I would like to thank Dr.Nather Basher, Ali Issam Hamodi for their assistance during my work . I present my thanks for AL-Nahrain University/College of science and all the staff members in the department of physics for their assistance. My special thanks for Miss Wasen who helped me a lot as a solid state laboratory member. Thanks for you all again, promising to help you in the future hopefully.

Israa

Abstract

The main problem is the replacing of Hg atom by covalent atoms such as (Cu,Sn) atoms in the compound $((\text{Hg}_{1-x}\text{A}_x)\text{Ba}_2\text{Ca}_2\text{Cu}_3\text{O}_{8+\delta})$ by consider $(x=0-1)$. Firstly, the high temperature superconductor of $(\text{HgBa}_2\text{Ca}_2\text{Cu}_3\text{O}_{8+\delta})$ Hg-1223 had been synthesized experimentally by solid state reaction. The high temperature superconductor $(\text{CuBa}_2\text{Ca}_2\text{Cu}_3\text{O}_{8+\delta})$ Cu-1223, $(\text{SnBa}_2\text{Ca}_2\text{Cu}_3\text{O}_{8+\delta})$ Sn-1223 had been synthesized by solid state reaction.

There are many parameters affected the preparation technique such as flow of oxygen, sintering temperature and compacted pressure. The ceramic samples of $(\text{HgBa}_2\text{Ca}_2\text{Cu}_3\text{O}_{8+\delta})$, $(\text{CuBa}_2\text{Ca}_2\text{Cu}_3\text{O}_{8+\delta})$ and $(\text{SnBa}_2\text{Ca}_2\text{Cu}_3\text{O}_{8+\delta})$ was analyzed by XRD technique to show the phase of Hg-1223. The XRD-pattern exhibited the presence of Hg-1223, Cu-1223 and Sn-1223 like tetragonal phase incomparable with the ASTM data sheet.

The analysis of XRD-pattern showed that the high phase Hg-1223 was predominated in the crystal structure of all compound $(\text{CuBa}_2\text{Ca}_2\text{Cu}_3\text{O}_{8+\delta})$ and $(\text{SnBa}_2\text{Ca}_2\text{Cu}_3\text{O}_{8+\delta})$. The XRD-pattern with the aid of a computer software to determine the lattice parameters. The lattice parameters for Hg-1223 were $a=3.99 \text{ \AA}$, $b=3.99 \text{ \AA}$ and $c=16.47 \text{ \AA}$, the compound Cu-1223 had $a=4.171 \text{ \AA}$, $b=4.171 \text{ \AA}$ and $c=16.743 \text{ \AA}$ and the compound Sn-1223 had $a=4.05 \text{ \AA}$, $b=4.05 \text{ \AA}$ and $c=15.682 \text{ \AA}$.

The EDX analysis for all compounds was investigated to show the elemental ratio in the mixture in agreement with the applied concentration of elements. The SEM analysis for all ceramic samples were showed the surface morphology and then the nature of grains and their size. The Iodimetric Titration Method also had been used to show the oxygen excess that was the role to enhance the mechanism of superconductivity.

The resistivity measurement plays an important role in proving the predominate phase and the superconductor behavior through the presence of

critical temperature which was about 115 K, 128 K and 110 K for superconductor compounds Hg-1223, Cu-1223 and Sn-1223 respectively. In order to remove the low phase Cu-1212 appearance in the crystal structure of the high temperature superconductor compound Cu-1223 and to improve the superconductor properties we repeated the sintering process. As a result the XRD analysis indicated that the low phase Cu-1212 predominated in the crystal structure which was had tetragonal phase with the lattice parameters $a=3.55 \text{ \AA}$, $b=3.55 \text{ \AA}$ and $c=12.37 \text{ \AA}$. The resistivity measurement was supported the low phase Cu-1212 with critical temperature about 64 K.

List of contents

Chapter one (overview on superconductivity)		1
1.1	Introduction	1
1.1.1	Application of Superconductor	1
1.2	History of superconducting	2
1.3	The Properties of superconductor	5
1.3.1	The critical temperature of superconductor	6
1.3.2	The critical magnetic field (B_c)	7
1.3.3	The critical current density	8
1.3.4	The isotope effect	8
1.4	The Meissner effect (complete diamagnetism)	9
1.4.1	Type I superconductors	10
1.4.2	Type II superconductors	11
1.5	The thermodynamic behavior	11
1.6	The BSC theory	15
1.7	The high temperature superconductors	17
1.7.1	Crystal structure of Hg-Ba-Ca-Cu-O System	18
1.7.2	The theory of high temperature superconductor	19
1.7.2.1	Interlayer coupling model	20
1.8	Literature review of Hg-Ba-Ca-Cu-O system	20
1.9	The aims of the project	34
Chapter two (experimental and procedure)		36
2.1	Introduction	36
2.2	Synthesis of $(Hg_{1-x} A_x) Ba_2 Ca_2 Cu_3 O_{8+\delta}$	36
2.3	The resistivity measurement	39
2.4	The structural properties	42
2.5	The Iodometric Titration method	43
2.6	Energy-dispersive X-ray and scanning electron microscope spectroscopy (EDS,SEM)	44

Chapter three (results and discussion)		45
3.1	Introduction	45
3.2	The Iodometric Titration results	45
3.3	Energy-dispersive X-ray spectroscopy (EDX)	46
3.4	The XRD analysis	48
3.5	Resistivity measurement	57
3.6	Crystallite size measurement	63
3.7	Scanning electron microscope (SEM) result	67
Chapter four (conclusions and suggested work)		69
4.1	Conclusions	69
4.2	Suggested works	69

List of Figures

Chapter one (over view on superconductivity)		
1.1	The historical event in superconductivity	5
1.2	The three parameters of the superconductor	6
1.3	Comparison between the normal conductor and superconductor in the resistance behavior	7
1.4	The magnetic field in normal and superconductor state	10
1.5	Type I and Type II superconductors in terms of magnetization and magnetic Fields	11
1.6	The transform of super electron to normal electron	13
1.7	Relation between penetration depth and temperature	14
1.8	The electron -lattice interaction	15
1.9	The schematic picture between the density of state $g(E)$ and E for the superconductor at $T=0$ the state is fully occupied	16
1.10	Crystal structure of mercury cuprate superconductor	18
Chapter Two (experimental and procedure)		
2.1	The cryogenic system for resistivity measurement	40
2.2	The relation between resistivity and temperature	41
Chapter three (results and discussion)		
3.1	The EDX pattern for Hg-1223 compound	47
3.2	The EDX pattern for Cu-1223 compound	47
3.3	The EDX pattern for Sn-1223 compound	48
3.4	The XRD pattern for Hg-1223 compound	49
3.5	The XRD pattern for Cu-1223 compound	51
3.6	The XRD pattern for Cu-1212 compound	54

3.7	The XRD pattern for Sn-1223 compound	56
3.8	The electrical resistivity for Hg-1223 compound	58
3.9	The electrical resistivity for Cu-1223 compound	59
3.10	The electrical resistivity for Cu-1212 compound	61
3.11	The electrical resistivity for Sn-1223 compound	62
3.12	The crystallite size and the non-uniform strain for Hg-1223 compound	65
3.13	The crystallite size and the non-uniform strain for Cu-1223 compound	65
3.14	The crystallite size and the non-uniform strain for Cu-1212 compound	66
3.15	The crystallite size and the non-uniform strain for Sn-1223 compound	66
3.16	The SEM for Hg-1223 superconductor compound	68
3.17	The SEM for Cu-1223 superconductor compound	68
3.18	The SEM for Sn-1223 superconductor compound	68

List of Symbols

The below list includes definition of the most symbols used in the thesis:

T_c	Critical temperature
J_c	Critical current density
B_c	Critical magnetic field
BCS-Theory	Bardeen-Cooper-Schrieffer theory
Bi-2223	$Bi_2Sr_2Ca_2Cu_3O_{10+\delta}$
YBCO	Yttrium barium copper oxide
HTSC	High temperature superconductor
MRI	Magnetic resonance imaging
IR	Infrared ray
EM	Electromagnetic
δ	Excess of oxygen content
amu	Atomic mass
M	Isotopic mass in (amu)
α	exponential of the isotope effect
$H_c(0)$	The magnetic field at zero Kelvin
χ_m	The magnetic susceptibility
μ_0	Vacuum permeability
M	Diamagnetic Magnetization
TBCO	Thallium barium calcium cooper oxide
Å	Angstrom
Hg-1223	$HgBa_2Ca_2Cu_3O_{8+\delta}$
Cu-1223	$CuBa_2Ca_2Cu_3O_{8+\delta}$
Sn-1223	$SnBa_2Ca_2Cu_3O_{8+\delta}$
ρ	Resistivity
w	Width of the sample
t	Thickness of the sample
l	Effective length between the electrodes

ρ^o	Normal resistivity
$T_{c\ on}$	Onset critical temperature
$T_{c\ off}$	Offset critical temperature
XRD	X-ray diffraction
λ	the wavelength of the (XRD) diffraction
θ	angle of diffraction
β	the full width at the half maximum
b	Crystallite size for Williamson and Scherrer
Ψ	the elastic strain
D	Crystallite size for Debye-Scherrer
K	Constant of Debye-Scherrer
EDX	Energy dispersive x-ray spectroscopy
SEM	Scanning electron microscope
C_v	Specific heat
J_s	The supercurrent density
n_s	Concentration of superelectron
λ_L	London penetration depth
n	Concentration of total conduction electrons
m	Electron mass
e	Electron charge
Δ_o	Energy gap

List of Tables

3.1	Variation of lattice constant , δ - Value, Volume of Unit Cell, T_c Value, and system with different samples (Hg-1223), (Cu-1223) and (Sn-1223).	67
3.2	Crystallite size and non-uniform strain by using Williamson-Hall method for Hg-1223, Cu-1223, Cu-1212, Sn-1223	69

CHAPTER ONE

Over view on superconductivity

1.1 Introduction:

The Superconductivity is one of the promising field in the material science application, there is a challenge to improve this properties during such new materials and compound. It is a macroscopic quantum phenomenon in a certain material when cooled below a certain temperature with zero resistivity and exhibiting the perfect diamagnetic behavior [1]. There were many theories and models explained this behavior but they were still incomplete to show the whole superconductor materials.

Later, the superconductor materials are classified into two type the conventional that is belong to BCS-theory and the unconventional one, which is not subjected to BCS-theory but other models like BCS-theory were applied [2]. Normally, there are two types of superconductor Type(I) superconductor for pure element exhibited ($T_c \leq 30$ K) and subjected to BCS-theory. Type(II) superconductor for alloys and compounds down at ($T_c \geq 30$ K) and does not classified by BCS-theory. There are many applications of cuprate based superconductor.

1.1.1 Applications of superconductor

1- Superconducting bulk.

There are many industrial applications have been done globally. The Superconducting bulk used to store electricity in a flywheel system because of its high capacity about 10 kw/h and could be operate safely for many months. On the other hand, that can be used as magnetic separation system for the water sterilization made by Hitachi company [2].

2- Superconducting motor for ships.

The propulsion system of the superconductor motor called “pod motor”, the propellers and the electric motor are directly connected so the design of the

boat is free and the possibility of the energy saving is occurred. The superconductor motor using Bi-2223 tape. The motor smaller and lighter than motors using copper wire [3].

3- SQUID

The SQUID system using Nb superconductor (Low temperature), YBCO superconductor (high temperature) and Hg-based superconductor (high temperature). The magneto cardiograph consists of SQUID system which is used for the diagnosis of human heart diseases [3].

4- The electric power transition.

The most important application of superconductivity is the transition of electricity from the electric station to cities by using HTSC cables. The HTSC Cables have lower Impedance, which are important for efficient transportation of Ac power [2].

5- Bio- magnetism

The Magnetic Resonance Imaging apparatus (MRI) that is used in medicine field. The magnetic field of the superconductor entered to the human body in order to detect the cells and tissues. Then the imaging and graph it on computer without needing a surgery [2].

6- Microwave device

There are many kinds of microwave device those were manufactured by cuprate based superconductor or any high temperature superconductor compound. It can be used to make an Infrared detection device. The detection occurs when cooper pairs destroyed by the absorption of IR photons and vanishing the superconductor behavior [2].

1.2 History of superconducting

The history of superconductivity was beginning with the experiment of Onnes in 1911, who was worked on the resistivity of metal at low temperature. Onnes used Liquid-He as a cooling medium in cryogenic system. He proved the

liquefaction temperature of He is 4.2 K. He used a Mercury rod to study the low temperature resistivity in order to conclude a residual resistivity (ρ_0) at zero kelvin. It was exhibited a zero resistivity at low temperature 4.19 K. He documented his results and he did not interpret this behavior. He classified this metal as a super metal and, later the behavior was called the superconductivity. After that, in 1912 Onnes was conducted an experiment on his result using superconductive ring to introduce an electric current inside it. The removing the battery he found that the intensity of the electrical current was still continue with the time. He was taking a Nobel prize at 1913 [4].

The understanding of superconductivity phenomena was appeared in the 1933 by Meissner and Ochsenfeld [5]. They observed that the superconductor sample was expelled the applied magnetic field, later it was known as Meissner effect. The brothers, F. London and H. London, in 1935 observed that the minimization of free energy carried by the superconducting current represented by the Meissner effect. In 1941, the first compound of niobium nitride superconductor showed T_c of about 16 K. The first macroscopic theory represented by the Ginzburg-Landau theory in 1950 [6]. They showed the presence two type superconductor, type (I) and type (II). In the same year, Maxwell [7] observed that the isotopic mass of the constituent element effected on the critical temperature of the superconductor and this is due to the electron-phonon interaction which is the microscopic mechanism of the superconductivity.

The understanding of the microscopic theory of superconductivity was completed by BCS theory that was suggested by Bardeen, Cooper and Schrieffer in 1957 [8]. The pairs of electrons which is interacting through the exchange of phonons called Cooper pairs. Kunzler et. al. in 1961[9] discovered that the compound SnNb_3 had a current density greater than 100,000 (A/cm^2) in the presence of magnetic of about 8.8 tesla. Berlincourt and Hake in 1962 observed that the alloys of niobium and titanium were useful for application at

magnetic field more than 10 tesla [10,11]. “Josephson Effect” was stated that the ohmic contact of two superconductor pieces that was separated by a thin layer of insulator there was a supercurrent can flow between them by the concept of tunneling effect. This prediction occurs in superconducting devices “SQUIDS” [12]. Later, the scientists directed their attention to ward high T_c value through the discovering a new compound and alloys.

The first compound of Lanthanum-based cuprate was showed a high temperature superconductor, it was discovered in 1986 by Bednorz and Muller [13]. They found that the transition temperature of about 35 K and it had perovskite structure. They were awarded the Nobel prizes in physics in 1987. After a short time Ching-Wu Chu found that the replacing of the Lanthanum with Yttrium atoms increasing the transition temperature to 92 K. The transferring from low temperature to high temperature superconductor was serve the technology during the application of liquid- N_2 as a coolant medium. That will save the energy in the application. The discovery of the superconductor compound YBCO ($YBa_2Cu_3O_{6+\delta}$) had very important sides where the liquid nitrogen could then be used as refrigerant where it can be produced cheaply and had no problems in piping like helium [14]. The superconductor compound Tl-Ba-Ca-Cu was discovered by Meada et.al. [15] with critical temperature 105 K in 1987. The first Hg compound HgBaCaCuO was synthesized in 1993 by Schilling et. al.[16] during the attempts to rise the critical temperature of the same compound. Chu et. al.[17] observed that using the pressure about 159 kbar during preparation rising the T_c above 150 K. The historical review and the expected development in future was explained in Fig. (1.1).

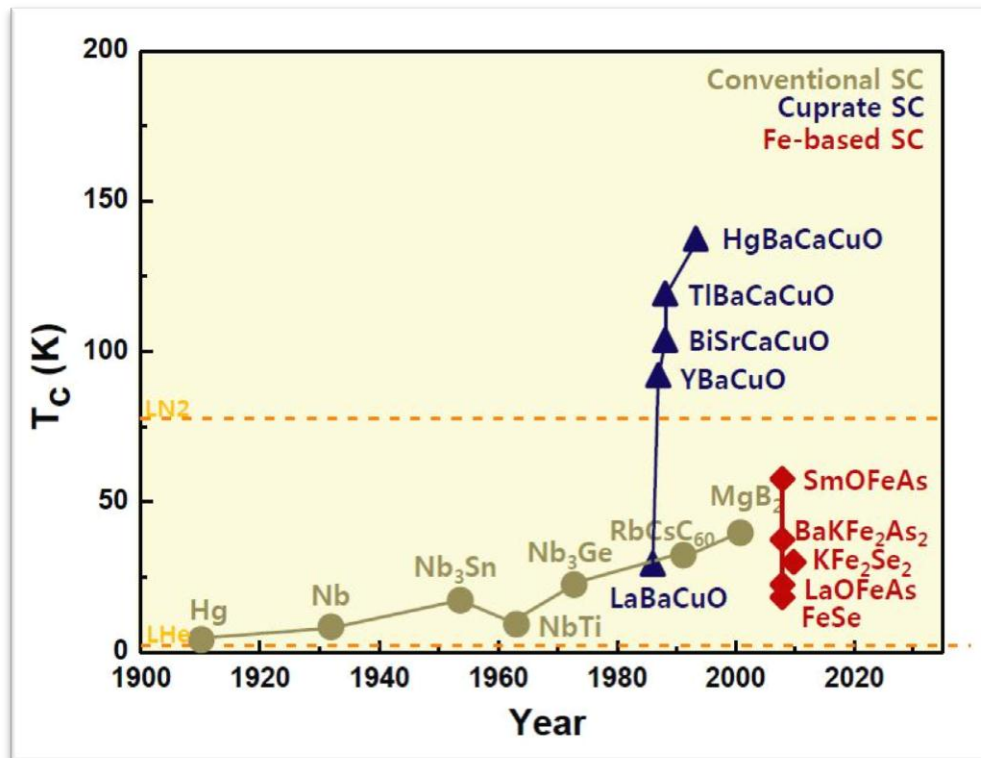


Figure (1.1); The historical event in superconductivity [18].

1.3 The properties of superconductor

The superconductivity is a phenomena describe by major and minor parameter. The major one can be represented by shielding parameter such T_c , H_c , J_c , as shown in Fig. (1.2). The other parameters are minor which are including by the major parameter. The main superconductor depends on the superconductor materials, such as the critical magnetic fields (H_c), the critical current density (J_c) and the critical temperature (T_c). The superconductivity described as a thermodynamic phase due to the previous properties which are independent to the microstructural details [18,19].

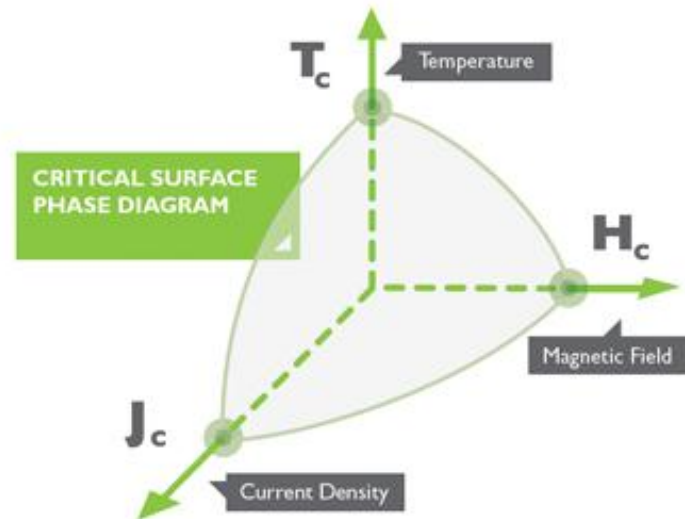


Figure (1.2); The three parameters of the superconductor [19].

1.3.1 The Critical Temperature of Superconductor

The critical temperature of the superconductor can be defined as the temperature required to make the resistivity (ρ) of a material reaches to zero. It is a temperature to change the phase from the normal phase to the superconductor phase, that is happened suddenly. The behavior of transition might take to form sharp or gradually decreasing in the resistivity. That depends on the purity of the materials. The transition from the normal to superconductor state is extremely sharp when the sample is pure. On the other hand, may be broadened when the sample is impure. The critical temperature depending on some parameters:

- 1- The condition of preparation.
- 2- The thickness of the sample.
- 3- The pressure during the synthesis.
- 4- The purity of the sample.

These parameters have a direct effect on the determination of the transition temperature of the material. The characteristics of zero resistivity in

the superconductor means that the resistivity of materials abruptly disappears at a certain temperature below the critical temperature T_c . The closed loop made from superconductor material would transform the DC current without any resistivity and losses. The maximum amount of resistivity in the superconductor state measured by the induced current experiment is less than ($10^{-27} \Omega \cdot m$). On the other hand, the maximum amount of resistivity in a good conductor state, such as copper is ($10^{-10} \Omega \cdot m$) at temperature equal to 4.2 K which is greater than the resistivity of the superconductor state. The relation between the resistivity and the temperature shows experimentally in Fig. (1.3) [20].

There is no dissipation of energy in the superconductor that is carrying DC current because the phonon does not scatter the charge carriers [2].

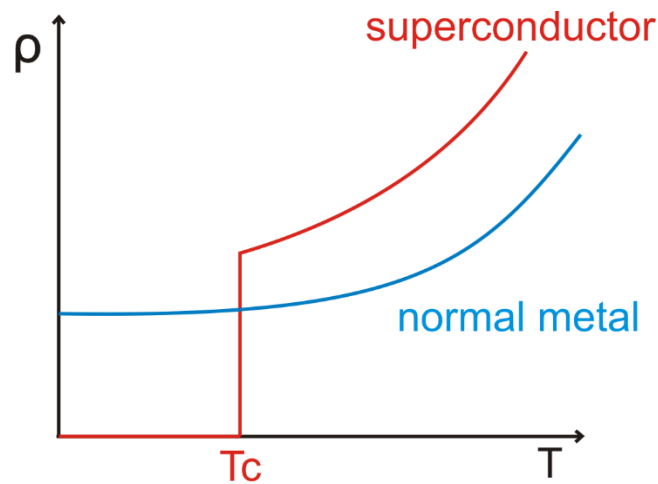


Figure (1.3); Comparison between the Normal Conductor and Superconductor in the Resistivity Behavior [20].

1.3.2 The critical magnetic field (H_c)

The second major parameter is the critical magnetic field H_c in conjunction with the critical temperature. The critical magnetic field H_c could be defined as the magnetic field strength in which above it the superconductivity destroyed. That means the flux density will penetrate the

sample without any interaction with the sample. Whereas below the critical field there is interaction of the flux penetrate with material and exhibiting the diamagnetic behavior. The critical temperature and magnetic field are associated with each other to form the superconducting state and related by the following relation [21,22].

$$H_{c(T)} = H_c(0) \left[1 - \left(\frac{T}{T_c} \right)^2 \right] \quad (1 - 1)$$

Where:

$H_c(0)$ - represented the magnetic field at zero Kelvin.

1.3.3 The critical current density

The major parameter, which are complement to the previous parameters, is the critical current density. It is produced as a result of critical magnetic field due to the concept of Lenz law in the right hand rule. It is used also to distinguish between the normal and superconducting phase and specified by (J_c). This current can be defined as the current in which above it the superconductivity destroyed. This current is establishing in the loop form for the sample under the magnetic field. It should be continuing under this condition because there is no resistivity appeared. These are the major parameters are strongly depending on the preparation method of superconductor material [23,24].

1.3.4 The isotope effect

One of the effects on the shielding parameter is the isotope effect. That is depending on the process of material formation, it has direct effect on the mechanism of the conducting and then the critical temperature T_c . For example, the transition temperature of the mercury decreases from 4.185 K to 4.140 K when the mass numbers of mercury change from 199.5 amu to 203.4 amu. The

dependence of the T_c is inversely proportional on the isotopic mass according to following equation [7].

$$M^\alpha T_c = \text{Constant} \quad (1-2)$$

Where:

α - is the exponential of the isotope effect.

M - is the isotopic mass in (amu).

The properties of the crystal lattice affected with the isotope mass where the ionic mass is related to the frequency of the lattice vibration [7].

1.4 The Meissner effect (complete diamagnetism)

The Meissner effect is one of the macroscopic experiences in superconductivity. This effect showed that if the magnetic field subjected to the superconductor material with $T < T_c$ then the magnetic flux completely excluded from the material and the inner field became zero as shown in Fig. (1.4b). On the other hand, the magnetic flux penetrated the material with no interaction at the normal state as shown in Fig. (1.4a). The superconductivity in the Meissner state when it had little or no magnetic field [5]. According to this equation:

$$B_{int} = B_o + \mu_o M \quad (1 - 3)$$

When

$$B_{int} = 0$$

$$0 = \mu_o H + \mu_o \chi_m H$$

$$\mu_o H(1 + \chi_m) = 0$$

$$\text{then } \chi_m = -1$$

In this case the superconductor material is becoming perfect diamagnetic [25,26].

Where:

χ_m - is the magnetic susceptibility.

M- is the diamagnetic magnetization.

M_0 - is the permeability.

The superconductivity breaks down when the applied magnetic field is too large. According to the previous fact of the critical magnetic field.

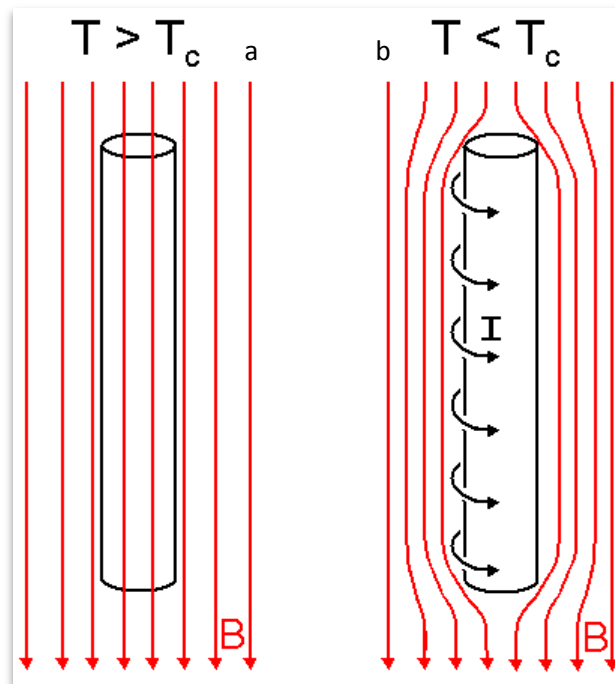


Figure (1.4); The magnetic field in normal and superconductor state [2].

1.4.1 Type I superconductors

The phase diagram between the magnetic field and the magnetization in type I superconductors represented as shown in Fig. (1.5a). This type has one value of the critical field $B_{(c)}$. When the external magnetic field above the critical value then there is a transition from the super state to the normal state.

This type mostly occurs on pure elements. Type I superconductor had approach to the perfect diamagnetism [27].

1.4.2 Type II superconductors

The phase diagram between the magnetic field and magnetization of type II superconductor as shown in Fig. (1.5b). There is two values of critical field, the lower critical field (B_{c1}) and upper critical field (B_{c2}). When the external magnetic field is less than B_{c1} , then the field excluded completely from it and behave like type I superconductor. When the external magnetic field increases above B_{c1} to B_{c2} then the flux partially penetrates into the superconductor as Vortices. Finally, when the field increased above (B_{c2}) then the flux completely penetrated through it and transferring to the normal state. Type II is more useful than type I because of the two value of the critical field including. This type mostly occurs in compounds and alloys [27].

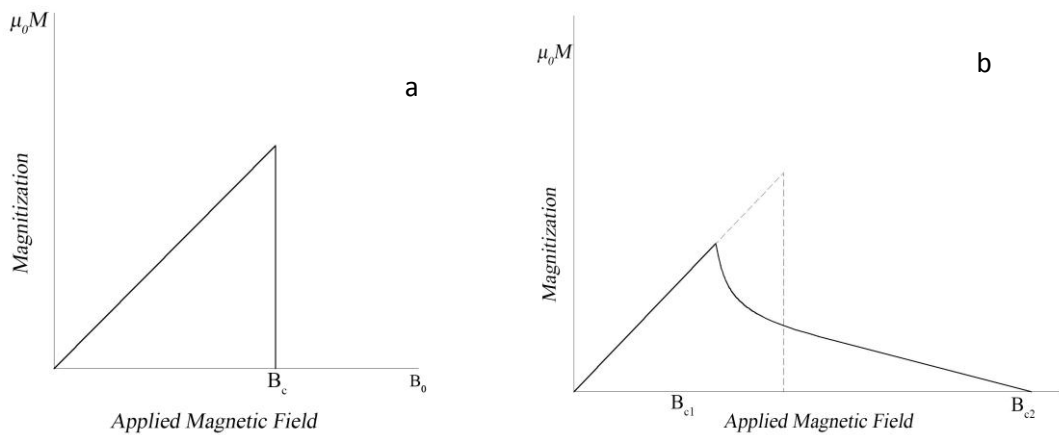


Figure (1.5); Type I and type II superconductors in terms of magnetization and magnetic fields [25].

1.5 The thermodynamic behavior

The thermodynamic aspect of superconductor explained that the specific heat of superconductor material decreases with temperature according to the relation [28].

$$C_v = ae^{-b\left(\frac{T}{T_c}\right)} \quad (1 - 4)$$

Where:

- a and b is a constants

The exponential term is related to the small energy gap in the spectrum of heat capacity. This gap lies in the range of fermi level, and it is a separation between the condensate state and normal state. The BCS theory was derived the concept of energy gap. The first theory was applied by Gorter and Casimir in 1934, they introduced the two-fluid model by giving the logic information on the thermodynamic properties of superconductor. They suggested that there are two types of conducting electrons, super electrons and normal electrons. The normal electrons describe the behavior of normal metal but the super electrons responsible for the properties of superconductor. The super electrons had zero entropy (no scattering) and long coherence length (about 10^4 \AA). The concentration of this electrons are depending on the temperature and applied by the following equation [28-30].

$$n_s = n \left[1 - \left[\frac{T}{T_c} \right]^4 \right] \quad (1 - 5)$$

Where:

n_s = Concentration of super electrons.

n = Concentration of total conduction electron.

When the temperature approach to (0 K) all electrons are super electrons, when the temperature increases these electrons transform to normal electron as shown in Fig. (1.6).

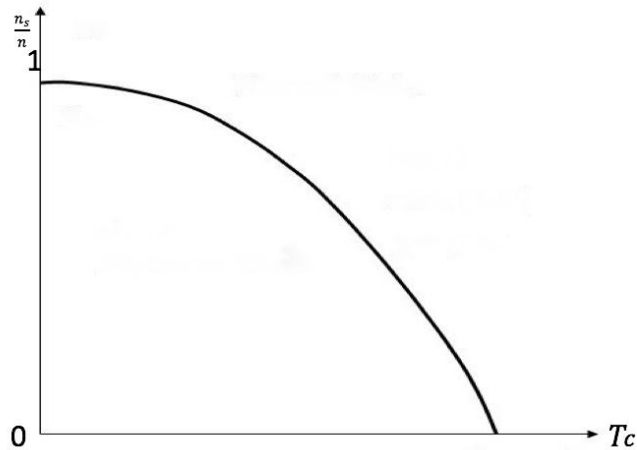


Figure (1.6); The transform of super electron to normal electron [28].

There is inversely proportional between the temperature and the small energy gap, when $T=T_c$ the gap will disappear and all electrons become normal electrons. The London equations stated by F. and H. London in 1935, they used the two-fluid model and applied the Maxwell equation to explain the electrodynamic properties. They concluded the following equations, which was related to B and J_s as follow [28-30].

$$B = -\left(\frac{m}{n_s e^2}\right) \nabla \times J_s \quad (1-6)$$

Where m represent the electron mass, e represent the electron charge and J_s represent the current density of free electrons.

This equation known as London equation. The solution of London equation gives:

$$B_y(x) = B_y(0) e^{-x/\lambda_L} \quad (1-7)$$

where the parameter (λ_L) means London penetration depth is define as [28-30].

$$\lambda_L = \lambda_L(0) \left[1 - \left(\frac{T}{T_c}\right)^4\right]^{-\frac{1}{2}} \quad (1-8)$$

$$\lambda_L(0) = (m/\mu_0 n_s e^2)^{1/2} \quad (1-9)$$

The above equations indicated that the magnetic field decreases exponentially from the surface to inside the superconductor with a limit penetration depth. This indication agrees with the fact that there is no perfect diamagnetic material as stated by the Meissner effect. The London penetration depth is varied with temperature by the following equation, such that at ($T \simeq T_c$), (λ) goes to infinity and the material goes to normal state as shown in Fig. (1.7).

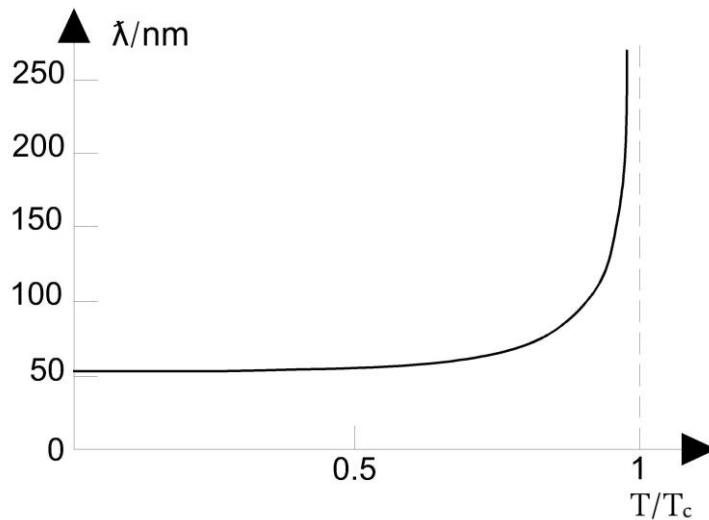


Figure (1.7); Relation between penetration depth and temperature [12].

There is an electric current flowing in region close to the surface and there is decay exponentially towards the center of the superconductor sample according to the following equation:

$$J_z(x) = -J_s(0)e^{-\left(\frac{x}{\lambda_L}\right)} \quad (1 - 10)$$

The result of the Meissner effect connected with this current where the magnetic field according to the surface current totally canceled the external field inside the medium resulting in a perfect diamagnetic of the superconductor [28-30].

1.6 The BCS theory

One of the most important theory in the superconductivity showed by Bardeen, Cooper, and Schrieffer in 1957 It was the first theory giving the logic interpretation of superconductivity concept. This theory was satisfied because it was explained all the phenomena of superconductor such as zero resistivity, energy gap and penetration depth. This theory was introduced the existence of the cooper pair. The cooper pair was defined as two electron interacted with each other to form the condensate state in the presence of phonon energy. The pairing transfer to independent electrons when the amount of energy applied to the system equal to the binding energy of the pair. On the other hand, if the binding energy is strong the superelectrons had opposite spins K' , K and opposite momentum. One can imagine the interaction of two electrons state the first electron was attracted to the ions which have positive charge (electron-lattice interaction). The second electron attracted to the first because the first screened by ions and shows a net positive charge. The cloud of phonons surrounding each electron, so the two electron interact with each other by exchanging this phonon as shown in Fig. (1.8).

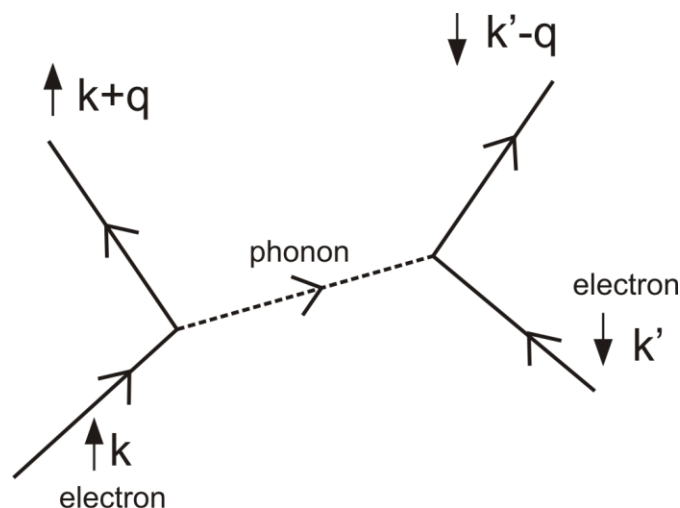


Figure (1.8); The electron-lattice interaction [25].

The cooper pairs had the same wave function form and the superposition of this pair defined as condensate state (the ground state of superelectrons). The presence of the cooper pairs is a function to produce the energy gap in the spectrum of fermi energy of electron as shown in Fig. (1.9).

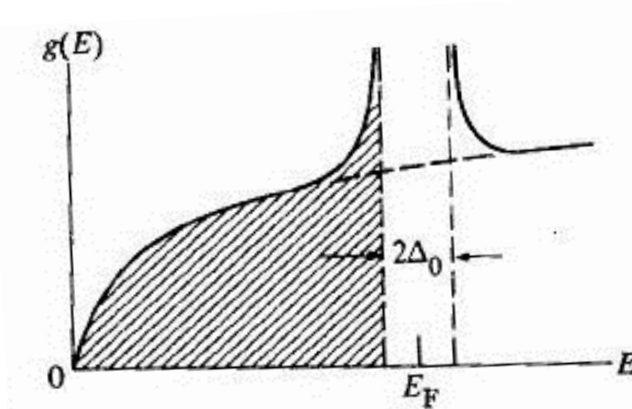


Figure (1.9); The Schematic picture between the density of state $g(E)$ and E for the superconductor at $T=0$ the state is fully occupied [28].

The BCS theory showed that the zero temperature producing the small energy gap is given by the following equation. It is clear that the small energy gap is a function to the value of (T_c) .

$$\Delta_0 = 3.52k T_c \quad (1 - 11)$$

Where Δ_0 represent the energy gap. This theory showed the isotopic effect on the behavior of superconductivity and then explained the zero-resistivity depending on the charge of isotopes. They showed the dependence of cooper pairs on the presence of energy gap and it may be destroyed if the energy applied is equal to $2\Delta_0$. This energy cannot supply by the phonon at low temperature because all phonon is in ground state for this reason the cooper pair continues to move without any resistivity [25,28,31].

1.7 The high temperature superconductors

The superconductor materials can be classified according to the transition temperature, if it was low critical temperature superconductor $T_c < 30$ K called low temperature superconductor. If the critical temperature T_c above 30 K it is called high-temperature superconductor that was first discovered by IBM research Muller and Bednorz [13] during their studies on the conductivity of the cuprate-perovskite ceramic (La-Ba-Cu-O). They found that the transition temperature was about 30 K, and they awarded the Nobel prize in physics [30,32].

This discovery made the researchers to find a new cuprate perovskite ceramic materials with higher transition temperature. They open the way to understand the physics of HTSC. They found that temperature of $(La_{2-x}Ba_xCuO_4)$ was increased with the application of the pressure [33]. Chu and Co-workers were working on new compound to increase the transition temperature to 92 K by replacing La atom by Y atom in nominal position $(Y_{1.2}Ba_{0.8}CuO_{4-y})$ [14]. After that many groups found that the compound $(YBa_2Cu_3O_{7-y})$ had T_c 90 K [34-36].

Meada et. al. [15]. studied the conductivity of Bi-Sr-Ca-Cu-O system prepared by solid state reaction then concluded the T_c value of about 105 K. Sheng and Hermann studied the superconductivity in TBCCO system prepared by SSR. had $T_c = 127$ K [37]. Later, the Hg-compound showed superconductivity in the $(HgBa_2CuO_x)$ compound, it had critical temperature of about 94 K [38]. The highest transition temperature was recorded in the compound $(HgBa_2Ca_2Cu_3O_x)$ of about 135 K due to the cuprate perovskite material [17], under high pressure the T_c increases to 164 K [39]. They are directing their attention toward the high temperature superconductor compounds reaching to the room temperature superconductor [40].

1.7.1 Crystal structure of Hg-Ba-Ca-Cu-O System

Actually, the new families of High T_c superconductor had a multiple perovskite structure[35]. The Perovskite structure is especial structure of cubic system, which is a combining of metallic elements and non-metallic elements, usually Oxygen. This structure consist of three chemical elements (A,B, and X), represented by the formula ABX_3 in their ideal form. The metallic cations, (the positive ion) represented by A and B the largest cation (A) lying in the center of each cube, and B-cation occupy all the eight corners of the cube. The nonmetallic anions, (the negative ion) represented by X and lies at the mid points of the cube edges. The crystal structure of the mercury cuprate superconductor is similar to the Tl-Ba-Ca-Cu-O superconductor, where Hg instead of Tl [38]. It has a multiple number of perovskite structure producing a tetragonal structure. This multiple is depending on the number of Cu-layer inserted in the mixture ($Hg Ba_2Ca_{n-1}Cu_nO_{2n+n}$). The parameter (n) denote the number of layer inserted in the unit cell. It had the value in the range (1-3) as shown in Fig. (1.10).

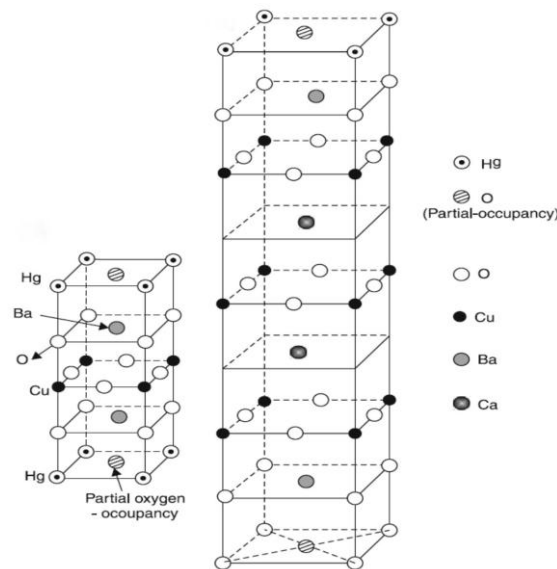


Figure (1.10); Crystal structure of mercury cuprate superconductor [2].

The tetragonal phase have lattice parameters equal to each other ($a=b$) and the Cu-distance in the plane had the value $\frac{a}{2} \cong 1.94 \text{ \AA}-1.93 \text{ \AA}$. The c-parameter is different from a,b and depending on the number of CuO_2 planes inserted. The superconductor compounds of Hg have four types of layers, The first type has (n) layer of (CuO_2) per unit cell and this layer separated by Ca layers with value (n-1) per unit cell. The CuO_2 and Ca- layers with each other forming the "conducting block". There are insulating slabs between two conducting blocks consist of HgO and BaO layers. The stacking sequence resulting in a rock salt type crystal structure [20].

The critical temperature is sensitive due to (n) layers producing the enlarging the structure of the compound. On the other hand, the experiments showed that T_c increases in Hg-1223 to 153 K under high pressure and high value of (n=3) [17]. Recently, there are many attempts to increase the T_c -value by increasing the Cu-O layers (n>3).They found there is no improvement in the T_c value, but it should be remain or decrease to low T_c -value [20]. That was return to the abrupt increasing in c-axis, which has a negative effect in the motion of carriers as like cooper pairs within the structure.

1.7.2 The theory of high temperature superconductor

The first theory of superconductivity had been devoted in low temperature mechanism, was BCS- theory, which were called the theories of conventional superconductor. The discovery of HTSC mads the physicists are going to explain the mechanism of superconductivity. Recently, there is no a common to explain the mechanism of high T_c superconductivity for all families and compounds. Many models had been done to explain HTSC, but the most satisfied called like-BCS theory, such as the interlayer coupling model.

1.7.2.1 Interlayer Coupling Model

The unconventional superconductor was considered as a stack of planar superconductors, which consist of conducting layers and insulating layers. It was assumed that the charges and spin dynamics in the CuO_2 planes are responsible for the properties of the normal and superconducting state of the high temperature cuprates. While the other layer in the crystal structure considered charge reservoirs. Which controls the charge density in the CuO_2 planes. The coupling in this model consists of two types, the interlayer interaction coupling and intralayer interaction based on BCS pairing theory by the superconductor layers.

The interlayer coupling is the interaction of the particle-particle channel plays a very important role in the enhancement of the transition temperature in the long range order of the oxide superconductor with respect to fluctuation. While the intralayer coupling interaction in the particle-hole channel plays a relatively minor role. The intralayer coupling interaction has effect on the hole density and gap parameter of the cuprate system. It was found that the magnitude of the interlayer hopping element and the critical temperature of the superconductor depends on the whole density between a two layer per unit cell. The supercurrent transfer along the c-axis between the CuO_2 layers (conducting plane) due to the interlayer hopping [20,29,41].

1.8 Literature review of Hg-Ba-Ca-Cu-O system

In this paragraph, it is necessary to discuss many researches that have been done locally and globally related to Hg-family. The purpose of this review is to show the position of our project with the previous researches and thesis. The specific review is mentioned to the researches dealing with physical properties of Hg-family superconductor and the covalent substitution that was dependent.

Dai et. al. [42] studied the effect of Tl substitution in Hg based-1223 phase superconducting compound. They found that the compound with the

formula $Hg_{0.8}Tl_{0.2}Ba_2Ca_2Cu_3O_{8+\delta}$ have transition temperature equal to 138 K due to the substitution with Tl. They used the neutron powder diffraction to find the crystal structure of this superconducting compound. They indicate the lattice parameters of the compound were $a=b=3.8489 \text{ \AA}$ and $c=15.816 \text{ \AA}$. pressure. They found that the sample $(Hg_{1-x}Tl_x)Ba_2Ca_2Cu_3O_{8+\delta}$ does not pure phase, it contains another phase which is $(Ca_{0.85}CuO_2)$ and $(CaHgO_2)$. They were observed that the substitution of Hg by Tl at $x=0.2$ in the superconductor compound $(Hg_{1-x}Tl_x)Ba_2Ca_2Cu_3O_{8+\delta}$ increasing the critical temperature from 135 K for Hg-1223 phase to 138 K for $(Hg_{0.8}Tl_{0.2})Ba_2Ca_2Cu_3O_{8+\delta}$ with extra oxygen 0.33.

Maigcan et. al. [43] prepared the superconductor cuprates $Hg_{0.8}V_{0.2}Ba_2CuO_{4+\delta}$, $Hg_{0.8}V_{0.2}Ba_2CaCu_2O_{6+\delta}$. Their work showed that there is a possibility to replace partially Hg by V in the two phases “1201” and “1212”. There was a difference between this two phases and the pure mercury based cuprate in the lattice parameters through the decreasing the c-parameter. They concluded that the substitution of vanadium in the site of mercury does not effect in the superconductor phases. The two samples had a narrow transition temperature at $T_c=90 \text{ K}$ for “1201” phase and $T_c=115 \text{ K}$ for “1212” phase.

Wang et. al. [44] studied the effect of F-doping in the superconductor compound Hg-Ba-Ca-Cu-O. The doping of F-ions had been applied at different temperature in the range (650 to 860°C). Their results were including the x-ray diffraction, Ac-susceptibility and resistivity measurement. The compound $HgBa_2Ca_2Cu_3O_{x-y}/F_y$ if ($y=0.0, 0.1, 0.2, 0.3, 0.4, 0.5, 0.6, 0.8, 1$ and 1.2) showed Hg-1212 phase rather than Hg-1223 phase. They were observed that there was no evaporation of mercury in the quartz tube in the presence of fluorine after sintering at 650 °C - 860 °C. While there was some evaporation of mercury in the quartz tube without fluorine after sintering. The previous result means that there was a strong interaction between mercury and fluorine. The XRD results showed that there were no impurities in the doped

samples with F ions. The doped compound of Hg-1212 phase had a lattice parameter less than the compound without fluorine. The last results mean that the F-doping causes a contraction of the unit cell. They concluded that the formation of the superconductor phase and the decomposition of the copper-oxide was accelerated by the F-doping. The fluorine atoms might be located at the O (3) site in the unit cell.

Lechter et. al.[45] was synthesized several members of high-temperature superconductors $(\text{Hg, Tl})(\text{Ba, Sr})\text{Ca}_{n-1}\text{Cu}_n\text{O}_x$ under high temperature and pressure by using a hot press. Their results showed that there were a multi phases and had a transition temperature of about 100 K. They observed that the superconductivity for the compounds Hg/Tl/Sr appears for single Tl-O and double Tl-O layers. Their results showed that the critical temperature was about 100 K for the 1212 phase. It may be the higher critical temperature due to 1223 phase. The compounds with double Tl-O layers 2212 phase showed high T_c between (70-80 K). The double layers of Tl-O are difficult to found in Tl/Sr without the substitution of Hg.

Tendeloo et. al. [46] prepared a new family of superconductor compound such as $\text{Hg}_{0.4}\text{Pr}_{0.6}\text{Sr}_2\text{CuO}_{4+\delta}$, $\text{Hg}_{0.4}\text{Pr}_{0.6}\text{Sr}_2(\text{Ca}_{1-x-y}\text{Sr}_x\text{Pr}_y)\text{Cu}_2\text{O}_{6+\delta}$ and $\text{Hg}_{0.4}\text{Pr}_{0.6}\text{Sr}_2(\text{Pr}_{1.7}\text{Sr}_{0.3})_2\text{Cu}_2\text{O}_{8+\delta}$. They studied the ordinary principles and defect structure by the electron diffraction and high resolution electron microscopy (HREM). They concluded that the distance between the (Pr,Hg) O_δ planes increases when (n) was increased and the correlation between them decreased. The ordered structure becomes more and more defective in the system (Hg,Pr)-Sr-(Sr,Ca,Pr)-Cu-O (1222) whereas the correlation is completely lost and it had triclinic unit cell. The structure of the compound $\text{Hg}_{0.3}\text{Pr}_{0.7}\text{Sr}_2(\text{Ca}_{0.4}\text{Sr}_{0.4}\text{Pr}_{0.2})\text{Cu}_2\text{O}_{6+\delta}$ was tetragonal phase such that the c-axis had a double value in the ordering between Sr and Ca layers. Finally, they indicated that this compounds due to its ordered superstructures were flexible in the substitution without changing their basic structure.

Du et. al. [47] studied the effect of the microstructure on the superconductor phase by the Pb-doped $Hg_{1-x}Pb_xBa_2Ca_2Cu_3O_{8+\delta}$ superconductor by the TEM analysis. The TEM result of $Hg_{0.66}Pb_{0.34}Ba_2Ca_2Cu_3O_{(8+\delta)}$ showed that the predominate phase was (Hg,Pb)-1223, the presence of two phases related to (Hg,Pb)-1234 and (Hg-Pb)-1212 phases. The two phase are usually extended one-unit cell along the c-axis. They studied the measurement of the current density (J_c) of the Pb-doped superconductor compound in the temperature range (30-60 K). They concluded that the current density of the Pb-doped sample is greater than the current density of the pure sample. It was increased from $10^5 Acm^{-2}$ to $10^6 Acm^{-2}$ in the Pb-doped sample. This increasing in the current density was due to the dislocations that was appeared in the Pb-doped mercury superconductor. This substructure was orthorhombic with lattice parameter $a=6.324 \text{ \AA}$, $b=2.807 \text{ \AA}$ and $c=10.573 \text{ \AA}$.

Chen et. al.[48] studied the relation between the superconducting transition temperature and the oxidation state of the superconducting compound $HgBa_2Ca_{n-1}Cu_nO_{2n+2+\delta}$ by the method of the bond-valence. The superconductor compound for (n=1-5) showed the full range of superconducting properties under optimally doped. They concluded that the maximum transition temperature depending on the number of CuO_2 planes per unit cell. They observed that the largest total mobile hole concentration was equal to (0.35) at (n=3). It was responsible for the highest transition temperature in the homologous series for the same value of (n).

Mandal et al .[49] prepared the compound $Hg_{0.7}V_{0.3}Sr_{2-x}La_xCuO_{4+\delta}$ at (x=0.1-0.8). The prepared sample contains mostly different impurity phases at (x=0). The partial substitution of La atom in the Sr site has a direct effect on the stability of Hg-1201 system. The XRD results showed that the crystal structure had a tetragonal phase with $a=b= (3.8133-3.8266 \text{ \AA})$ and $c=(8.7361-8.7944 \text{ \AA})$. They concluded that the samples showed a metallic behavior when

the resistivity varied with the temperature. The sample with ($x = 0.5$) producing a small amount higher - T_c phase $T_c \sim 87$ K during annealing in Ar at 340 °C for 4 hr. The critical temperature of the previous results was close to the critical temperature of the optimally doped compound $HgBa_2CuO_{4+\delta}$ was 94 K. They concluded that as-prepared samples in the atmosphere was quite stable over long period without losses of the superconducting properties. They found that all samples had been a relation between T_c and Cu-O(1), a Cu-O(2) bond lengths.

Tatsuki et. al.[50] studied the superconductor properties of the prepared superconductor compound (Hg,Tl)-2223 and (Hg,Tl)-2234 . They synthesized the compound $(Hg_{1-x}Tl_x)_2Ba_2Ca_{n-1}Cu_nO_y$ for $n=3,4$ under high pressure and temperature with ($x=0.3-0.6$). They observed that the phase stabilization of (Hg,Tl)-2223 showed increasing in T_c within the range (45 to 81 K) at ($x=0.3-0.6$). The effect of annealing under Ar tend to increase T_c to 90 K. The increasing of critical temperature was due to the reduction of hole content in the CuO_2 sheets. The changing in critical temperature was accompanied with increasing in c-axis.

Yao et. al.[51] was studied the intergrowth phenomenon in Hg-Ba-Ca-Cu-O superconductor system after synthesized under high pressure for long time. They prepared the superconductor phase Hg-2435 under high-pressure and high temperature by solid state reaction. They studied the variety of intergrowth in the superconducting phase Hg-2435 by the high resolution electron microscope in order to conclude the long period phase of Hg-2223 superconductor. He concluded that the two phases Hg-2435 and Hg-2223 contain only Hg-1212 and Hg-1223 phases. The superconducting phase Hg-2435 consisted one layer of Hg-1212 phase and one layer of Hg-1223 phase. The critical temperature of Hg-2435 phase was 135 K. The Hg-2223 phase consist three layers of Hg-1212 phase and one layer of Hg-1223 phase with c-

axis equal to 6.68 nm. They concluded that for $n > 3$ there was no Hg-1234, Hg-1245 and Hg-1201 phases.

Tholece et. al. [52] studied the properties of the mercury based superconductor compound. They found that the critical temperature of the formula $HgBa_2Ca_{n-1}Cu_nO_{8+\delta}$ was reaching to (135 K) for ($n=3$). The critical temperature was increased to maximum value versus the oxygen content and in the range ($1 < n < 5$).

Chmaissem et. al. [53] prepared the superconductor compound $Hg_{1-x}Cr_xBa_2CuO_{4+\delta}$ with ($x=0$ to 0.27). The structure of chromium was tetrahedral coordinate with four oxygen atoms. Two of these atoms moved to new position and the others in the Hg/Cr plane. On the other hand, the four atoms of extra oxygen showed a tetrahedral coordination around each Cr atom. The $Hg_{1-x}Cr_xBa_2CuO_{4+\delta}$ samples were metastable under a surrounding condition and this is why the carrier concentration cannot controlled under low temperature oxygen annealing. They were concluded that T_c values were decreased when the chromium increased. The benefit of the annealing showed the phase separation, decomposition, and superconductivity is irreversible destroyed.

Antipov et. al. [54] studied the effect of the extra oxygen on the structure and superconducting properties of Hg-1201 compound. They found that the extra oxygen was calculated by the Iodometric titration method and neutron powder diffraction (NDP). They showed that the extra oxygen located in the middle of the Hg mesh only. They were concluded that the optimal value of δ in the range (0.08-0.12) for Hg-1201 phase. Their results had a good agreement with the traditional mechanism which is 2δ holes per (CuO_2) layer.

Karpinski et. al. [55] introduced a summary on the crystal growth of the superconductor compound Hg-12(n-1) for ($n=1-5$) that was synthesized under high gas pressure. It was difficult to control the Hg, HgO and O_2 partial pressure in order to get non stoichiometric composition. They studied the

crystal growth of the (Hg,Pb)-1201 phase and they found that the undoped crystal had a full occupancy of Hg position (97%) with $T_c = 94$ K. The doped crystal had a substitution up to 10 % with $T_c = 80$ K. The x-ray diffraction showed that there is a shifting in the position of the mercury and oxygen atoms due to the Pb-O bonds.

Sastry et. al. [56] studied (Hg,Bi) $Ba_2Ca_2Cu_3O_y$ by using a series of quenching experiments. The sample that had the formula $Hg_{1.0}Bi_{0.2}Ba_2Ca_2Cu_3O_y$ or $Hg_{1.0}Bi_{0.2}Ba_2Ca_2Cu_{3.1}O_y$ prepared by using solid state reaction. Two different source of Hg was used for the preparation, internal Hg-source and external Hg-source. They found that the sample with external Hg-source (HgO) showed a porous micro structure with small grains that was similar to the internal Hg-source. On the other hand the samples with external Hg-source ($CaHgO_2$) have a superior microstructure with large regions of aligned plat like crystals of (Hg,Bi)-1223 phase. The magnetization measurement indicated that the superconductor prepared by using external Hg-source had a wider hysteresis than the superconductor that prepared by the internal Hg-source. The transition temperature for all samples were in the range (130-134 K). They concluded that the phase purity of the sample and the microstructure was developed in (Hg,Bi)-1223 phase depending on Hg-pressure and heat treatment.

Lokshin et. al. [57] prepared Hg-1234 and Hg-1245 phase by high pressure, high temperature technique and study the characterization of overdoped phase. They observed that the preparation of Hg-Ba-Ca-Cu-O system was very sensitive to synthesis condition. The critical temperature T_c was changed from overdoped state (116K in Hg-1234 and 100K in Hg-1245) to underdoped state (95 K in Hg-1223 and 85 K in Hg-1245) and, finally to optimally-doped state (125 K in Hg-1234 and 111 K in Hg-1245). This change was due to the heat treatment under nitrogen or oxygen flows. They concluded that the critical temperature of the sample depends on conductivity and oxygen

content. They observed that the large value of $(n>3)$ exhibited a cupola shape in T_c value. They observed that the compound $HgBa_2Ca_{n-1}Cu_nO_{2n+2\delta}$ had the same structure arrangement with extra oxygen for $(n>3)$. They concluded that the heat treatment caused a variation in a carrier concentration in Hg-1234 and Hg-1245 samples.

Pandey et. al. [58] studied the effect of Tl substitution on the microstructure of the superconductor compound $Hg_{1-x}Tl_xBa_2Ca_2Cu_3O_{8+\delta}$ where $(x=0.2, 0.4, 0.5, 0.6, \text{ and } 0.8)$. They observed that the resistivity measurement showed the variation in the critical temperature from 106 K to 133 K for underdoped sample and from 106 K to 129 K for the overdoped samples. The transition from the underdoped to overdoped region was took place when Tl have a range between 0.5 and 0.6. The XRD and TEM analysis observed that the samples have a multiphasic of Tl-1223.

Acha et . al .[59] studied the effect of the pressure on the critical temperature of the superconductor compound $Hg_{1-x}Au_xBa_2Ca_2Cu_3O_{8+x}$. They concluded that not only the change of the transfer charge between the reservoir blocks and the copper oxide plane effect on the critical temperature but there is another effect by pressure. They concluded that the large T_c of Hg-1223 phase was due to the coupling between CuO_2 blocks due to the contraction of the Hg layers under pressure. There was a stability of high critical temperature under pressure. Chemical substitution should be done in order to reduce the distance between the CuO_2 blocks.

Yom et al .[60] was synthesized two compounds $Ca_{2-x}Hg_xCuO_y$ and $Fe_{1-x}S$ by using high pressure (56 GPa) and mechanical alloying method, respectively at $(x=0.1, 0.2)$. The two sample was showed abnormal resistivity which was ranging (150~ 254 K).

Valldor et. al.[61] prepared the superconductor compound $Tl_{2-x}Hg_xSr_2Ca_1Cu_2O_z$, at 880 °C from metal oxides. Two samples were

prepared with $x=0.7$ by solid state reacton in closed ampoules and by single crystal growth at a high pressure furnace. There is a similarity between the two samples in the critical temperature which was equal to 45 K. On the other hand, there is a difference between the two samples by the impurities. The single crystal sample was homogeneous 500 μm in size. The cell parameter for the solid state parameter due to higher content of Sr had larger than single crystal sample. The EDS results showed that some copper atom entered in the (Tl,Hg) site during the high pressure synthesis, forming the composition $(Tl_{0.8}Hg_{0.7}Cu_{0.5})(Sr_{1.7}Ca_{0.3})Ca_{0.7}Sr_{0.3}Cu_2O_{7.5}$. The XRD results revealed that Sr and Ca sites had mixed occupancies and the larger site for Sr.

Orlando et. al. [62] prepared superconductor compound (Hg,Re-1223) that had the formula $Hg_{1-x}Re_xBa_2Ca_2Cu_3O_{8+\delta}$ with $x = 0.05$. This sample was prepared with the help of thermobaric analysis technique that kept the total pressure inside the quartz tube during the preparation at high temperature. The sample was examined by XRD and ac susceptibility measurement. The synthesis of the single phase Hg,Re-1223 had been investigated by the variation of O_2 content and the filling factor of the mercury was about 0.014 gcm^{-3} . They found that the superconducting phase enhanced when the O_2 reduction in the sample $(Re_{0.05}Ba_2Ca_2Cu_3O_{8+\delta})$, and the mercury partial pressure increased inside the quartz tube. The resistivity measurement was showed increasing in the transition temperature. They investigated that there is no equivalent between the external hydrostatic pressure and chemical Re doping in the compound $Hg_{1-x}Re_xBa_2Ca_2Cu_3O_{8+\delta}$ for $(0 < x < 1)$. While there is a similarity in the reduction of the lattice volume induced by chemical pressure and external hydrostatic pressure for Re doping $(0 < x < 1)$.

Kim et. al. [63] prepared the sample $Hg_{0.8}Tl_2Ba_2Ca_2Cu_3O_{8+\delta}$ using the high pressure, high-temperature technique. They found that cooling process during the synthesis of the sample effected on the quality of the sample and the

preparation condition. The XRD result of $Hg_{0.8}Ti_{0.2}$ -1223 had increasing the c-axis and an important change in the a-b plane comparing with Hg-1223. They observed that there is no difference in the XRD result between sample prepared by quenched precursor and the furnace cooled precursor.

Celotti et al. [64] found a new cubic phase Cu-free sample ($Hg_2Re_{0.5}Ba_4Ca_{1.5}O_{8.5}$) with a diamond-like diffraction pattern during the improvement of the preparation method in sealed quartz tube with Re-doped (Hg-1223) superconductor. The determination of the crystal structure showed the atomic coordination was closely similar to $Ba_4CaCu_3O_{8.25}$ with a difference on the position of the heaviest cations. The lattice constants were about (8.48 Å–8.53 Å) according to the length of the thermal treatment. They were considered that the new phase was singularly Cu-free and does not show superconductivity more than impurities during the successful synthesis of Hg(Re)-1223.

Sedmidubsky et al. [65] studied the phase relations in Hg-Ba-Ca-Cu-O system. They examined the stability regions of the phase diagram (P_{Hg}, P_{O_2}, T) in the selected sections for Hg-1212 and Hg-1223. The phase stability diagram was studied for Hg-1212 and Hg-1223 at 800 °C. They observed that the stability of Hg-1212 phase were lying on the $BaCuO_2 - CaO$ tie-line with low P_{Hg} . They found that there is no stability of Hg-1223 phase between (500-800 °C). This low stability might be to the inexact data used during the calculations. The phase was stabilized due to the formation of some defect like vacancies, or Cu on Hg position.

Giri et al. [66] studied the effect of cationic size and the microstructural properties of the superconductor compound $Hg(Tl/Bi)Ba_2Ca_2Cu_3O_{8+\delta}$. They prepared the polycrystalline samples by solid state reaction. The samples had the form $HgBi_{0.2-x}Tl_xBa_2Ca_2Cu_3O_{8+\delta}$ with (x= 0.00, 0.05, 0.1, 0.15, 0.2) corresponding to the phase 1223. They found that the average dopant radius R_d effected on the superconducting properties and stability of the 1223- phase. The scanning electron microscopy SEM showed that the samples had average dopant

radius differs significantly from the Hg radius. The dense of microstructure and the grain alignment consequently is in the form of a large plate-like. They concluded that the transition temperature was sensitive to the average dopant radius. They explored that $HgBi_{0.15}Tl_{0.05}Ba_2Ca_2Cu_3O_{8+\delta}$ had a maximum critical temperature of about 131 K with average dopant cation size 1.108 Å and critical current density of about ($1.29 \times 10^3 A/cm^2$) at 77 K.

Lokshin et. al.[67] synthesized the superconducting compound $(Hg_{(1-x)}Cu_x)Ba_2Ca_2Cu_3O_8$ for ($0 \leq x \leq 0.8$) at temperature equal to 900 °C. They found that the samples containing more than 95% of the phase Hg-1223. The critical temperature for all samples was found to be 135 K. They suggested that the synthesis of the samples required high synthesis temperature and low partial pressure.

Batista-Leyva et. al.[68] studied the resistive transition of the superconductor compound $(Hg_{0.85}Re_{0.15})(Ba_{1-y}Sr_y)_2Ca_2Cu_3O_{8+\delta}$ with $y=0, 0.17, 0.2, \text{ and } 0.28$ at different magnetic fields. They found that the Sr-substitution responsible for the improvement of transport properties. The resistivity measurement taken in the range 130-300 K. They found that the interlayer distance was increased with the Sr content. They suggested that the Sr-substitution improve the phase HgRe-1223 HTSC polycrystalline for transport application.

Kandyel.[69] synthesized the superconductor compound $(Hg_{1-y}Tb_y)Sr_2(Tb_{1-x}Ca_x)Cu_2O_{6+\delta}$ with ($y \approx 0.5$), ($0 \leq x \leq 0.8$) The prepared samples studied by EDX and X-ray diffraction. The results showed that the Tb ions was important for the stabilization of the compound $(Hg_{1-y}Tb_y)Sr_2TbCu_2O_{6+\delta}$ at $y \approx 0.5$. The electrical resistivity and magnetic susceptibility measurement for $(Hg_{0.5}Tb_{0.5})Sr_2(Tb_{1-x}Ca_x)Cu_2O_{6+\delta}$ showed the substitution of Tb by Ca was necessary. The x-ray diffraction result indicated that the samples with $x=0.5$ had less Cu-O planes than the sample with Ca-free

$(Hg_{0.5}Tb_{0.5})Sr_2TbCu_2O_{6+\delta}$. The samples became superconductor when ($x > 0.2$). The critical temperature increased when the content of Ca increased and the highest critical temperature was about $T_c = 88$ K at $x = 0.8$.

Giri et al. [70] studied the effect of Bi-substitution with the Hg site in the mercury cuprate superconductor at ($n=3$) corresponding the general formula $Hg_{1-x}Bi_xBa_2Ca_2Cu_3O_{8+\delta}$ with $x=(0.005, 0.10, 0.15, 0.020$ and $0.25)$. They found that the critical temperature in the range (118-128 K), the highest T_c for $(Hg_{0.95}Bi_{0.05})$ -1223 sample. The result of XRD and electron microscope investigation reveal that all samples were polycrystalline and having a tetragonal phase of (Hg,Bi)-1223 with a minor impurity phase $BaCuO_2$ and (Hg,Bi)-1234. They concluded that the highest transport critical current density was with formula $(Hg_{0.85}Bi_{0.15})$ -1223 was equal to 1.05×10^3 A/cm² at 77 K. While the lower critical current density was about 6.35×10^2 A/cm² for the compound $Hg_{0.95}Bi_{0.05}Ba_2Ca_2Cu_3O_{8+\delta}$. They found that the c-axis had linear decreasing when Bi increased while the a-parameter was stable. The relation of Bi-substitution with c-parameter reveal that the Bi cations was full incorporation in the structure.

Zehetmayer et. al. [71] studied the effect of neutron and electron irradiation on superconducting $HgBa_2CuO_{4+\delta}$ single crystals. They measured the magnetic moment in the superconductor compound Hg-1201 phase by SQUID magnetometer. They found that the electron and neutron irradiation used to modify the defect structure. The two type of radiation affected the irreversible properties.

Kandyel [72] synthesized and studied structure, transport properties of the superconductor compound (Hg,Fe)-1212. He used the sealed quartz tube method to prepare $(Hg_{1-y}Fe_y)Sr_2(Y_{1-x}Ca_x)Cu_2O_{7-\delta}$ ($y=0.5, 0 \leq x \leq 1$) compounds. He investigated the lattice parameters, resistivity measurement, dc magnetic susceptibility, oxygen content, thermoelectric power and copper

valence as a function of Ca content (x). The XRD results indicated that both Fe and Y are necessary for the stabilization of (Hg,Fe)-1212 compound. He found that the critical temperature increased from 30 K to 82 K for ($x=0.3-0.6$) and decreasing from 82 K to 69 K for ($x=0.6-0.8$). The previous results revealed that the doping state of the samples varied from underdoped to overdoped states by the Ca substitution. Finally, the measurement of the oxygen content showed that the copper valence for the sample with $T_c=82$ K was 0.8 and different from 2.02 to 2.26 with increasing x from 0 to 0.8.

Corsini et. al.[73] studied the superconducting properties of Sm and In doping in the $HgPb_2$ compound. The microstructure of the compound observed by scanning electron microscopy SEM. The phase composition analysis by using Energy Dispersive Spectrometry EDX. The XRD analysis indicated that the compound $HgSm_{1-x}Pb_2$ had a tetragonal phase. The substitution of Sm atoms in the Hg vacancies does not effected the onset critical temperature of $HgPb_2$ phase. The results of the x-ray diffraction of the compound $HgSm_{1-x}In_xPb_2$ for ($0.2 < x < 0.7$) had pseudo-cubic structure that had a lattice constant equal to 4.88 Å.

Orlando et. al.[74] prepared the polycrystalline samples ($Hg_{0.82}Re_{0.18}Ba_2Ca_2Cu_3O_{8+d}$) with three value of oxygen content. They determined rhenium valence and local oxygen coordination in these samples by using rhenium edge x-ray absorption spectroscopy, they found that the rhenium valence varied from (+6.8, +6.9 and +0.7) as a function of oxygen content in these samples. The extending x-ray absorption fine structure measurement revealed that the local oxygen ordered around Re atoms which was indicated the ReO_6 octahedron distortion for all samples. The results from the thermoelectric power showed a small increasing in the number of a charge carrier as a function of oxygen content.

Possos et. al. [75] investigated a small resistive device based on the ceramic compound $Hg_{0.8}Re_{0.2}Ba_2Ca_2Cu_3O_{8+\delta}$ in order to improve this in future and found a prototype for protecting systems with low impedance and high current system. Their initial study showed that the a fault current $1.55 \times 10^2 A/cm^2$ at 60 Hz decreased to $0.82 \times 10^2 A/cm^2$ without any damage on the superconductor (Hg,Re)-1223 used in this device.

Alias et. al. [76] synthesized the high temperature superconductor compound Hg-1223 by solid state reaction method. They found that the optimum sintering temperature was 860 °C for 200 hr with heating and cooling rate of 1 °C/min. They prepared the high temperature superconductor compounds with a nominal composition $Hg_{1-x}In_xBa_{2-y}Sr_yCa_2O_{8+\delta}$ for ($0 \leq x \leq 0.5$) and ($0 \leq y \leq 0.5$). The results shown that the In doping reducing the sintering time to 150 hr. The XRD analysis indicated that the crystal structure of the samples was tetragonal phase with high- T_c phase (1223) and low- T_c phase (1212) in addition to the existing of impurity phases.

Babych et. al. [77] prepared of Pb, Fe and Cd doped Hg-1223 superconducting copper oxides by using sol-gel method to prepare Hg-free precursor $Ba_2Ca_2Cu_3O_{8+\delta}$. In their work, they carried out the synthesis of 15% Pb, 5% Fe and 5% Cd doped Hg-1223 HTSC. They found the superconducting and impurity phases for all samples by the determination of scanning electron microscopy and microprobe analysis. They found that the Hg,Fe,Pb-1223 compound possessed high density and non-superconducting phases such as $HgCaO_2$ and $BaCuO_2$. Also, the critical temperature for Hg,Fe,Pb-1223 samples were equal to 129 K and 118 K respectively. The critical temperature for Hg,Cd-1223 sample was 126 K.

Mendonca et. al. [78] synthesized the high temperature superconductor compound Hg-1223 by using the combustion method. They prepared sample at

(1.8 GPa) with $T_c = 132$ K. The results indicated that Hg-1223 was a tetragonal phase with lattice parameter ($a=b=3.8721$ Å and $c=15.7283$ Å) with space group P_{4mmm} . Result from the magnetization measurement showed a double transition at 130 K and 102 K which could be attributed to the presence of secondary phases.

Jabar [79] prepared the HTSC compound of $Bi_{2-x}Hg_xSr_{2-y}Ba_yCa_2Cu_3O_{10}$. The substitution percentage of Hg and Ba are (0, 0.05 and 0.1) the sample prepared by a solid state reaction. He synthesized the compound as pellet and wire. The critical temperature of samples measured by using four points probes techniques. He found the substitution of Sr. by Bi had low critical temperature samples. The XRD results, showed the compounds were an orthorhombic structure. The samples doped with Ba showed an increasing of the c-parameter compare with barium free sample. He found that the volume fraction change due to the change in the concentration of Ba and Hg.

1.9 The aims of the project

The literature review was a benefit to have a knowledge on the high temperature superconductor compound like $HgBa_2Ca_2Cu_3O_{8+\delta}$. It was found that Hg-1223 compound was an important compound due to its high critical temperature. Previously, there was only Tl-1223 family derived from Hg-1223 family and no one made a full substitution with Hg atoms by covalent atoms in order to improve Hg-family and saving the single phase Hg-1223, this is the reason why we suggest this project. The steps of this project were done by the following statement.

- 1- The preparation of superconductor compound $HgBa_2Ca_2Cu_3O_{8+\delta}$ will be done by solid state reaction method.

- 2- The crystal structure of the compound $HgBa_2Ca_2Cu_3O_{8+\delta}$ will be analyzed by using special software to find the lattice parameter, the symmetry, particle size and their distribution in the comparison with data base related to the program.
- 3- The replacing of Hg atoms by Cu and Sn ions in the compound ($Hg_{1-x}A_xBa_2Ca_2Cu_3O_{8+\delta}$) by considering (x=1) to produce a novel phase like Hg-1223 family such as Sn-1223 and Cu-1223 high T_c superconductor phases in order to improve the properties of the superconductor compound.
- 4- Studying the effect of the new systems by physical properties like XRD-analysis, resistivity measurement, Energy dispersive spectroscopy EDS, Scanning electron microscope SEM.
- 5- The expected result will tell us the ability to produce the new phase of high T_c superconductor derived from Hg-1223 phase. The new phase will be considering the new one in the field of superconductivity especially there is no one worked on the production of those new phases depends on the literature review. For this reason, the data will be obtained needs more and clear definition in the classification of Cu-1223 and Sn-1223 as a high- T_c superconductor.

CHAPTER TWO

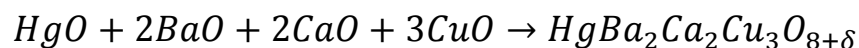
Experimental and Procedure

2.1 Introduction:

This chapter is dealing with the synthetic method for Hg-family superconductor materials. The techniques those were used to give a complete explanation of the prepared samples. The technique that was used to prepare Hg-family superconductor is solid state reaction. It was considered the most widely synthetic method to prepare a ceramic material from the mixture consists of the solid materials. This reaction had been done at high temperature below the melting temperature of the mixture. There is a suitable rate required to show the interaction. The main problem in this project is the replacing of Hg element by other covalent atoms such as (Cu,Sn) atoms in the compound $(Hg_{1-x}A_x)Ba_2Ca_2Cu_3O_{8+\delta}$ by consider (x=1) in order to prepare a new family Cu-1223 and Sn-1223 related to Hg-1223.

2.2 Synthesis of $(Hg_{1-x}A_x)Ba_2Ca_2Cu_3O_{8+\delta}$

First of all, it was necessary to concentrate our attention on the synthesis of $HgBa_2Ca_2Cu_3O_{8+\delta}$ superconductor compound by consider (x=0). The Hg-1223 compound was synthesized by the solid-state reaction using by the roots of HgO, BaO, CaO, and CuO with high purity and appropriate weights according to the chemical reaction.



Since Hg element will evaporate from the nominal composition before reaction with other oxide. Then the synthesis was normally carried out in a sealed quartzes tube by the following steps:

1. The precursor with a nominal composition is starting by BaO, CaO, CuO to produce the composition $Ba_2Ca_2Cu_3O_8$. They were mixed and

weight for each reaction by using a sensitive balance with 4-digit type STATION 462AL.

2. The gate mortar was used to mix the powders of BaO, CaO, CuO with each other for (50-60) min. The powder was homogeneity by adding some drops of high purity 2-propanol to form a paste. This process was repeated for many times.
3. The drying of the resultant powder was necessary to remove the humidity from the mixture. It was used the oven at temperature 150 °C for half hour.
4. Then, the dried powder put in the furnace by (alumina crucible). It was calcined in a flow of oxygen with atmosphere pressure rate 0.5 l/min in a tube programmable furnace at 850 °C for 24 hr. The heating and cooling rate was about 80 °C/hr. The flow of oxygen was necessary for the extra of oxygen in the mixture and change the compound from stoichiometry to non-stoichiometry.
5. The dark black powder was mixed with the mercury oxide (HgO) and regrinding again to form the composition $HgBa_2Ca_2Cu_3O_{8+\delta}$.
6. Then, the dried powder is pressed into a pellet by 1.5 cm in diameter and 3 cm thick. The electrical press (CARVAR) type was used at pressure (0.509 GPa). The mechanical pressing is an important process used to reduce the porosity in the pellet during the sintering process. That was an important step during the preparation of the sample for all measurement and analysis.
7. Then the pellet put in a sealed quartz tube evacuated using rotary pump to get a pressure of 10^{-2} mbar. The pellet was place in a tube programmable furnace and sintering with a heating rate 60 °C/hr up to 600 °C for 1 hr and up to 850 °C for 10 hr with the heating rate equal 60 °C/hr. Then the furnace was cooled down to 550 °C for 1hr with a

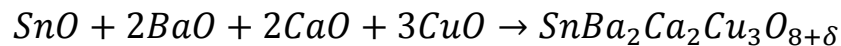
cooling rate 60 °C/hr and cooled down to the room temperature at the same cooling rate. The sintering process is necessary to form a dense ceramic body under a high suitable temperature below the melting temperature to liquefaction [80]. The temperature controlling during the sintering is very important to get the high density of the pellet. This factor is important to increase the grain-boundary diffusion and volume diffusion depending on the temperature. The size and distribution of particles in the composition was also concluded.

8. The second step of the project is the full substitution of Hg atoms by Cu and Sn atoms at $x=0$ according to the relation $(Hg_{1-x}A_x)Ba_2Ca_2Cu_3O_{8+\delta}$.
9. The new system of Cu -1223 was synthesized by the solid state reaction by using the materials CuO, BaO, CaO , with an appropriate weight in proportion to their molecular weights according to this reaction.



The preferred method was done by using the same above steps. The calcined powder was pressed into a pellet with 1 cm in diameter and 3cm thick by using the CARVAR electrical press with a pressure equal to (1.066 GPa) and then sintered. the pellet in alumina crucible with flow of oxygen. The pellet was sintered with flow rate of oxygen equal to 0.5 l/min at 900 °C for 24 hr. and the heating rate was about 45°C/hr. The pellet was cooled to the room temperature with the cooling rate 40°C/hr. The sintering process was repeated to improve the physical properties of Cu-1223 compound.

10. On the other hand, the producing of Sn-1223 compound was synthesized by the solid state reaction by using the materials SnO, CuO, BaO, CaO, with an appropriate weight in proportion to their molecular weights according to the following reaction by the replacing of Hg-ions by Sn-ions.



The preferred method is done by depending the previous steps.

The calcined powder was pressed into a pellets with 1 cm in diameter and 3cm thick by using the CARVAR electrical press with a pressure equal to (0.764 GPa).

Then the pellet was put in alumina crucible, the sintering process was done in a flow of oxygen. The pellet was sintered in flow rate of oxygen equal to 0.5 l/min at 900 °C for 24 hr and the heating rate equal to 45 °C/hr. The pellet was cooled to the room temperature by the cooling rate 40 °C/hr.

11. The resistivity measurements had been done on the prepared samples to show the presence of high temperature superconductor or not, especially it was a new family derived from Hg-1223 family.

2.3 The resistivity measurement

The resistivity measurement is one of the most important analysis used to prove the existence of superconductivity of the prepared sample. The normal metal has the linear relation between the resistivity and temperature, but in the super state there is abruptly decreasing in the resistivity goes to zero defining the superconducting state. The closed cycle cryogenic system of liquid helium is used under vacuum of about 10mbar to determine the critical temperature (T_c) of the sample by using four probe technique as shown in Fig.(2.2).

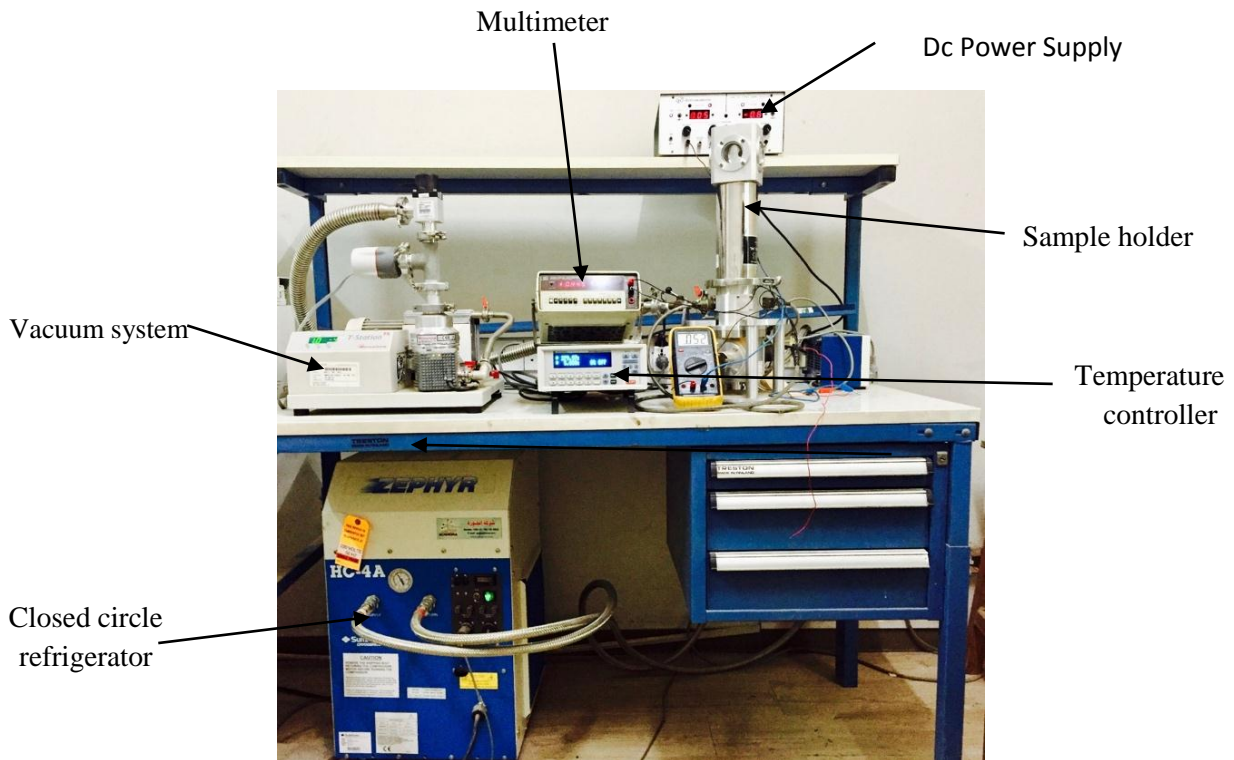


Figure (2,1); The cryogenic system for resistivity measurement.

The Silver paste was used during the measurement to connect the sample under the four probe technique. Two for current and the other two for voltage. The D.C. power supply was used to supply the sample with the constant current and the voltage was measured by a digital nano voltmeter type (Keithely), which had the sensitivity about ($\pm 0.1 \mu V$).

Then the resistivity was measured according to the following equation [81].

$$\rho = \frac{V}{I} * \frac{wt}{l} \quad (2-1)$$

Since the current (I) was passing through the sample and the voltage drops across the electrodes.

Where:

W: Represents the width of the sample.

t: Represents the thickness of the sample.

l: Represents the effective length between the electrodes.

The relation between the resistivity and temperature occurs graphically as in Fig. (2.3).

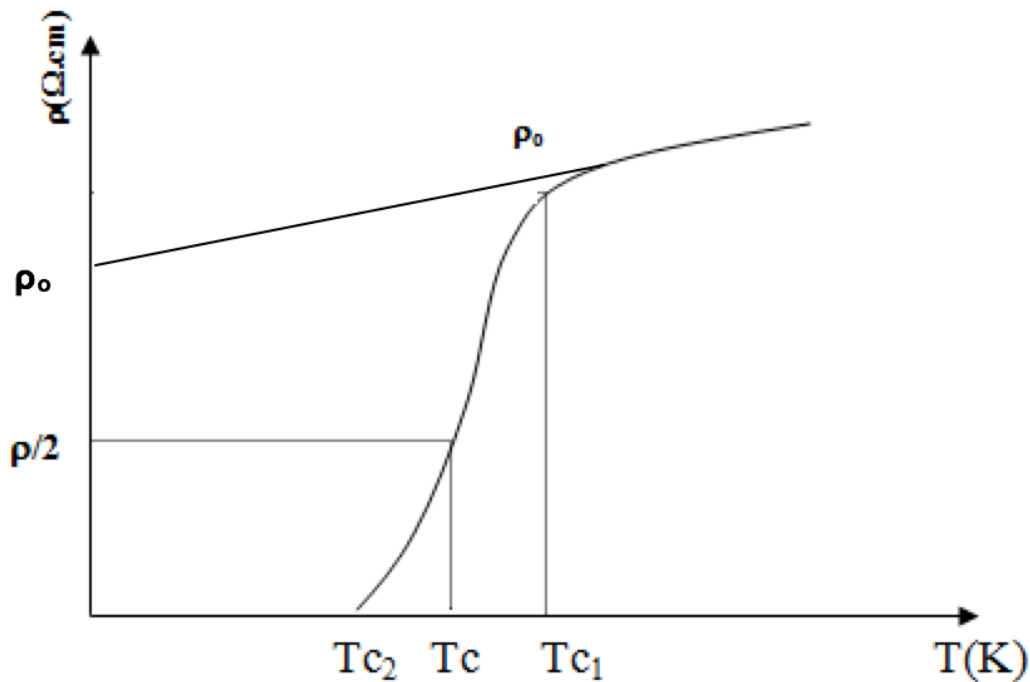


Figure (2,2); The relation between resistivity and temperature.

The tangent to normal resistivity is extended and intercepts the y-axis to determine the residual resistivity (ρ_0) at 0 K. Then taking the half value of (ρ_0) to determine the temperature value that meets the half value of ρ_0 . This is the critical temperature. Secondly, the temperature that intercepts ($0.9\rho_0$) is defined as the onset temperature (T_{con}). Thirdly, the meeting point of temperature and ($0.1\rho_0$) is defined as the offset critical temperature (T_{coff}). Finally, the tendency of zero resistivity at a certain temperature is called the zero temperature (T_{c0}). The best superconductivity occurs within the value of ΔT_c in the range (1-10 K). The value of (ΔT_c) is measured by the difference between T_{con} and T_{coff} ($T_{con} - T_{coff}$). The narrow region of (ΔT_c) is better than the wide region of (ΔT_c). That is, the return to preparation method that is applied.

2.4 The structural properties.

The structure of the prepared samples was studied by using X-ray diffractometer XRD at the room temperature. The type of device was used (Philips) had the source $\text{CuK}\alpha$ with wave length ($\lambda=1.5405 \text{ \AA}$), the current applied to 30 mA and the voltage 40 kV. There are two type of analysis that were investigated from XRD-pattern. The first one related to crystal structure such as the lattice constants and the angle between them. The second one give more details about the nature of crystal structure. The required software was used type High score and refine to get the above information. Normally, these software depends on the principle following equation:

$$2d \sin\theta = n\lambda \quad (2-2)$$

$$d = \frac{1}{\sqrt{\frac{h^2}{a^2} + \frac{k^2}{b^2} + \frac{l^2}{c^2}}} \quad (2-3)$$

The parameter (d) is the inter planer distance, (θ) is the angle of diffraction, $\lambda(n)$ is the order of diffraction and (λ) is the X-ray wavelength. The second analytical type are dealing with particle size and their distribution. It was used to obtain the particle size by Williamson and Scherrer method:

$$\frac{\beta \cos\theta}{\lambda} = \frac{0.89}{b} + 4\Psi \frac{\sin\theta}{\lambda} \quad (2-4)$$

Where (β) is represent the full width at the half maximum(FWHM), (b) is represent the crystallite size, (Ψ) is represent the elastic strain. The thing is mention to complete all these analysis by using a scientific software called X-powder to determine all information related to crystal structure through the lattice constant (a,b and c) the symmetry, particle size and their distribution depending on the required data base related to this software.

2.5 The Iodometric titration method

It is a chemical method that was used to determine the amount of oxygen excess (δ) during the synthesis of the cuprate superconductor. It was measured by the chemical process. This method could be summarized by this steps.

1. Taking the mass of the sample powder of about (40-45 mg) and grinding, then put it inside a conical flask on the magnetic stirrer.
2. The solution was added to the powder that is consist of 1.25 ml (10%) HCl and 2.5 ml of saturated KI (3.17 g of KI with 2.5 ml H_2O). The color change of the liquid is dark brown due to the producing I_2 .
3. Sodium thiosulfate solution $Na_2S_2O_3$ with a concentration of about 0.015 g/ml (0.3g of $Na_2S_2O_3 \cdot H_2O$ in 20 ml of H_2O) was added to the liquid gradually until turning the color from dark blue yellow, then the reaction is finish. During the addition when the color of the liquid turned to low brown drops of starch adding to the solution.
4. The volume of the titrated $Na_2S_2O_3$ solution was measured. The content of the oxygen could be measured by the following equation [82].

$$\delta(O_2) = \frac{\frac{M_A}{M_B} - \frac{3m_A}{cv}}{\frac{2m_A}{cv} - \frac{M_o}{M_B}} \quad (2 - 5)$$

Where (M_A) is represent the molar masses of the sample, (M_B) is represent the molar masses of $Na_2S_2O_3 \cdot 5H_2O = 284.1$, (m_A) is represent the weight of the sample~ (40-450) mg, (C) is represent the concentration $Na_2S_2O_3 = 0.015$ g/ml , (V) is represent the volume of $Na_2S_2O_3$ used in the titration and (M_o) is represent the atomic weight of oxygen.

2.6 Energy -dispersive X-ray and scanning electron microscope (EDX,SEM).

The important technical analysis is Energy-dispersive X-ray spectroscopy EDX which is used to determine the ratio of the elements in the compound and compare the result with the XRD result of the sample to show the compatibility of the two results [83]. The device made by Bruker company, Germany. Morphological was studied by the scanning electron microscope SEM (made by FEI company, Netherlands, inspect S50). The SEM is analytical technique imaging the surface of the sample by focusing the electrons beam on the atoms of the sample. Several SEM photos are taken for a bulk samples in order to show the particle size distribution, the grain size and the nature of particle distribution through the homogeneity.

Chapter Three

Results and Discussion

3.1 Introduction

The successive preparation of the samples ($HgBa_2Ca_2Cu_3O_{8+\delta}$), ($CuBa_2Ca_2Cu_3O_{8+\delta}$) and ($SnBa_2Ca_2Cu_3O_{8+\delta}$) by solid state reaction were translated into a specific result to specifying the superconductor behavior of above samples. These results were obtained by X-ray Diffraction XRD, Iodometric Titration Method, electrical resistivity measurement, scanning electron microscope SEM, energy-dispersive x-ray spectroscopy EDX, and particles size.

3.2 The Iodometric titration result.

The Iodometric titration is a chemical experiment of Iodin. It is used to measure the amount of extra oxygen (δ) in the sample that was pumped during the sintering process. The extra oxygen is an important factor during the synthesis to form the superconductor phase by transferring the compound from the stoichiometry to nonstoichiometric. This experiment based on the release of the Iodine during the chemical reaction. The amount of the extra oxygen is calculated from the equation (2-4). The experiment showed that the δ -value for the Hg-1223 compound was about 0.07. That means the number of the oxygen content per unit cell was about (8.07). The δ -value for Cu-1223 compound was (0.1). That mean the number of the oxygen content per unit cell was about (8.1) and the δ -value for the Sn-1223 was about (0.22) as mentioned in Table. (3-1). That means the number of the oxygen content per unit cell (8.22).

It was clear that the extra oxygen for Sn-1223 compound was greater than Cu-1223 and the Hg-1223 compound. The location of the extra oxygen was taking the center of the basal planes in the perovskite structure. The basal planes

were linked the whole structure and proved by the XRD analysis. The high extra oxygen atoms might be the reason to high T_c -value because that is related to the coupling between the layers, which were increased in Cu-1223 compound by increasing the extra oxygen.

3.3 Energy-Dispersive X-ray Spectroscopy (EDX).

EDX was considered one of the important tools that give us an information about the ratio of the elements composed the compound. The EDX pattern for Hg-1223 compound, Cu-1223 compound, and Sn-1223 compounds have been shown in Fig. (3.13-15) respectively below. The ratio of the elements obtained from the EDX was compared with the ratio that was dependent in the synthesized by the chemical reaction. It was founded that the ratio of the elements was approached to the theoretical value of the chemical reaction. Normally, the ratio of oxygen was not clear because it is a light atom. It was clear that the new high- T_c families like Cu-1223 and Sn-1223 phases were investigated by the coincidence of elemental ratio with the applied one during EDX-analysis. It was clear that the compound Cu-1223 and Sn-1223 were formed as the style of Hg-1223.

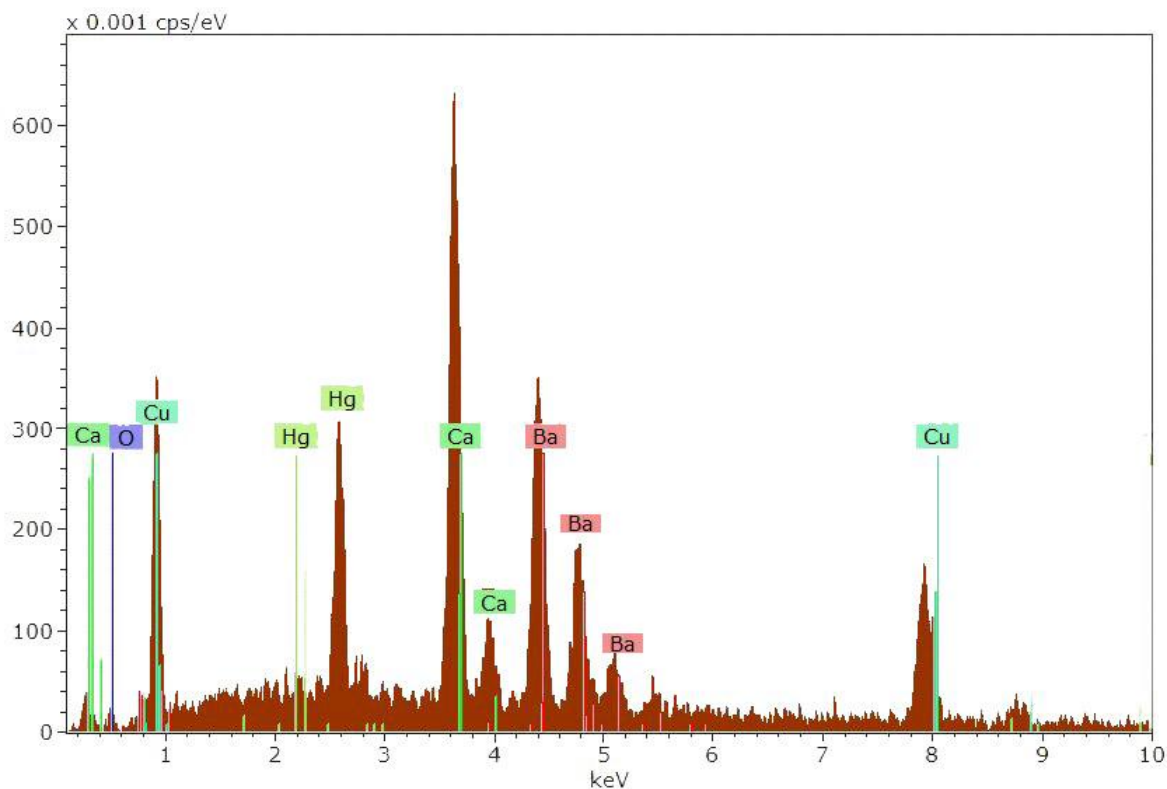


Figure (3.1); The EDX pattern for Hg-1223 compound.

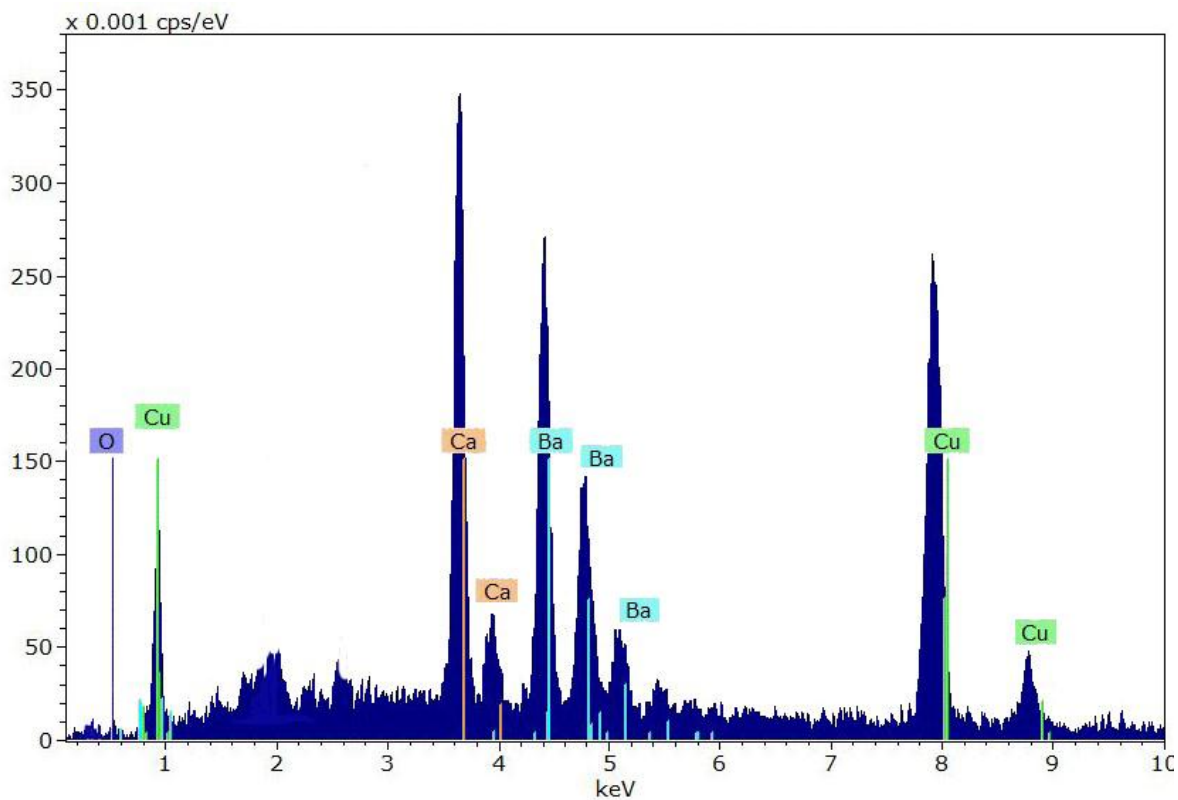


Figure (3.2); The EDX pattern for Cu-1223 compound.

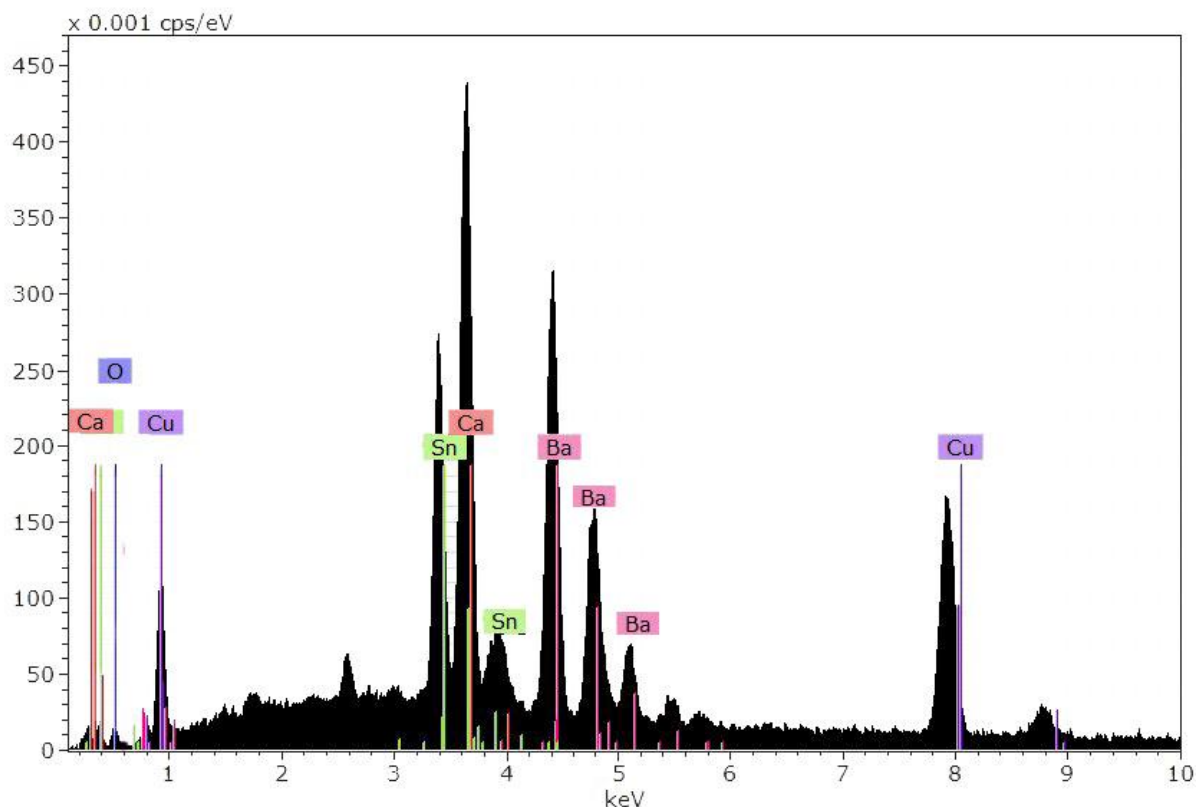


Figure (3.3); The EDX pattern for Sn-1223 compound

3.4 The XRD analysis.

The XRD analysis was used to study the formation of the structure phase required in comparable with the data base. The properties of a required phase is including the lattice constants (a,b and c), the space group, the partical size and the strain occurs in the structure. These properties were studied using the software Crystal Impact Match V3.2.1, Crystal Diffract V.6.0.5, Refine Lab and x-powder. The study included the pure Hg-Ba-Ca-Cu-O sample and then the full substitution of Hg by Cu, Sn. The aim of this step was to determine the change in the structure phase after the full substitution.

The XRD analysis indicated that the crystal structure was tetragonal phase with lattice constant $a=b= 3.855 \text{ \AA}$ and $c= 15.847 \text{ \AA}$. The synthesized sample with a long length of sintering at $850 \text{ }^\circ\text{C}$ by the solid state reaction as mentioned before caused the small difference in the lattice constant. Besides, the

appearance of the low phase Hg-1212 in our result that formed by the ratio 16% of the whole structure played an important role in the lattice parameters. Our results were approximately similar to what was done by Isawa et. al. they prepared nearly similar superconducting phase of Hg-1223 by using encapsulation method [84]. The XRD pattern for the high temperature superconductor compound ($HgBa_2Ca_2Cu_3O_{8+0.077}$) have been appeared in Fig.(3.1).

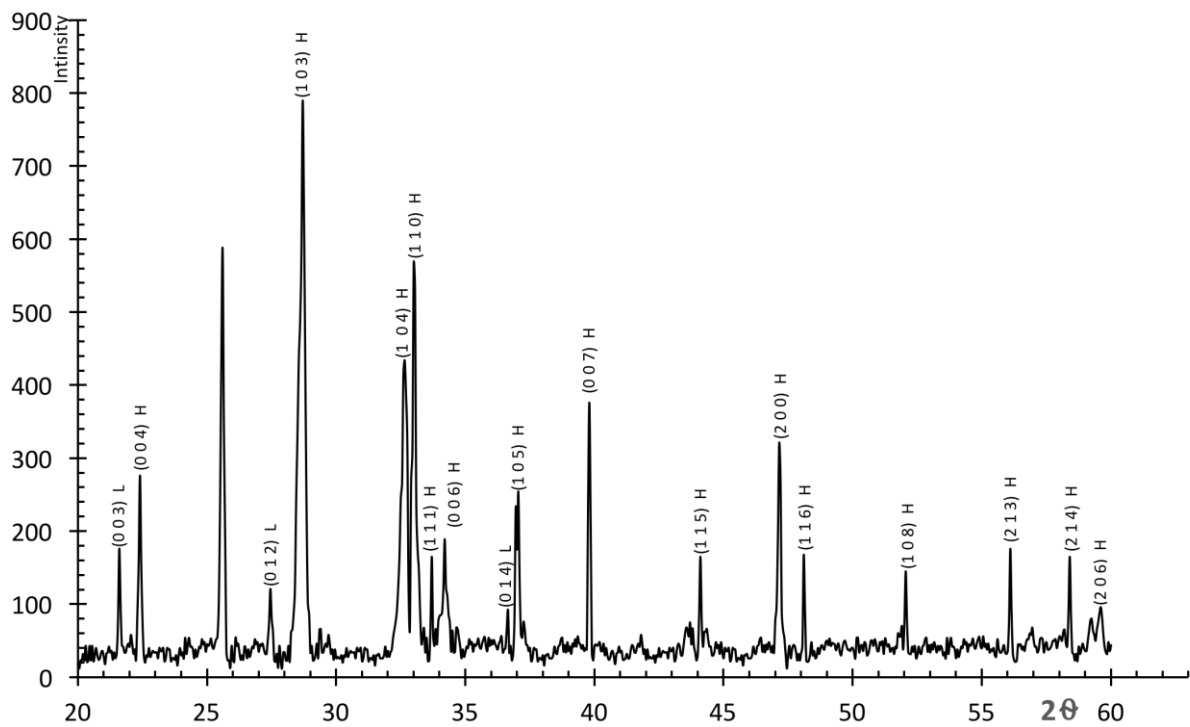


Figure (3.4); The XRD pattern for Hg-1223 compound.

The appearance of different peaks was remarked to the presence of multiphase of Hg-1223. Some of these peaks were related to high phase superconductor Hg-1223 and the others were related to low phase. The most peaks were belonging to the high phase more than the low phase superconductor Hg-1212. The ratio of high phase formation was about 84% of the whole peaks appeared. This result was agreed with the resistivity measurement that will be

discussed later. In general, the appearance of a single high phase of Hg-1223 rather than the low phase was the reason to show the predominate high phase in the XRD pattern. The peak positions of low phase were represented by ($2\theta=21.56, 27.41$ and 36.61) and accompanied to hkl-planes were (003), (012) and (014) respectively. The low phase of Hg-1212 was compared with the international centre for diffraction data (ICDD) with the pdf file (98-007-4104) [85]. The position of the peaks gives more details on the plane due to this diffraction. Whereas the intensity of the peaks is related to the concentration of this plane in the multiperovskite unit cell. The shifting in the peaks might be related to the change in the lattice constant in comparison with a standard one.

There was two peaks in the structure related to hkl (110) and (200) at 2θ equal to (32.96) and (47.11) respectively. I think the first peak (110) was including the basal plane and satisfy the symmetry for all the unit cell. It was necessary to form the bond O-Hg-O. The second plane (200) linked the extra oxygen in the perovskite structure and the number of atoms per unit cell in the plane (110) is more than the plane (200). This is the reason why the intensity of (110) was greater than the plane (200). The presence of the plane (200) was remarked to oxygen extra in the unit cell. The planes mentioned by (102), (103), (104), (105), (108) and (206) at ($2\theta=25.56, 28.67, 32.61, 37.01, 52.01$ and 59.56) respectively. These layers may make the connection between the inserting layer or acting as steps within the unit cell to transmit the moving of charge carriers through the principle layers in the direction of b-c axes. The principle plane (004) formed the Cu_2O bond, whereas the planes (006) and (007) formed the (O-O) bond. These planes varied in intensity because of the different activities of those planes under diffraction.

The highest intensity of the peak (103) at ($2\theta= 28.67$) was return to the principle diffraction within the unit cell. It was considered that this plane act as step between the layer in the b-axis. The Refine program was applied to find the

lattice constant and then structure phase. It was found that there was a tetragonal phase with $a=b$ 3.99 Å and $c=$ 16.47 Å. The result agreed with the data sheet (ICDD) (98-004-1652) [86]. The small difference between the lattice constants might be attributed to the small shifting in the peak positions (2θ). This shifting perhaps coming from the extra oxygen that takes a position in the basal plane. The results of Williamson method showed the strain value of about ± 0.3 , this is proof for the extending or shrinking in the lattice constant in comparison with previous results. On the other hand, this strain is a function also to the temperature during the measurement of the XRD. Normally, this result agreed with the data of Iodometric Titration, that would be discussed later. The XRD pattern for full substitution Cu-ions with respect to Hg-ions is mentioned in Fig. (3.2). Producing the new phase Cu-1223 related to Hg-1223 high- T_c superconductor phase.

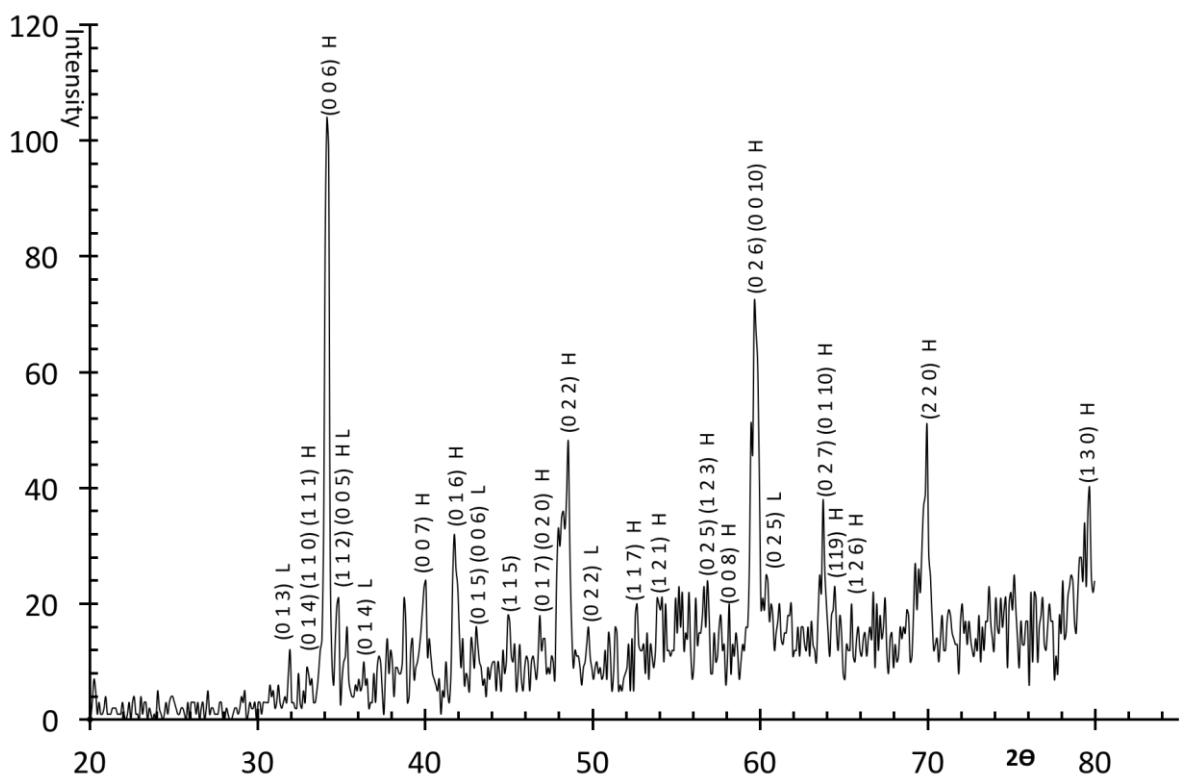


Figure (3.5); The XRD pattern for Cu-1223 compound.

The obtainable result of the compound ($\text{CuBa}_2\text{Ca}_2\text{Cu}_3\text{O}_{8+\delta}$) showed that the presence of the peaks related to high superconductor phase Cu-1223 was

more than the low phase superconductor Cu-1212. The ratio of high phase was about 74% of the whole structure. This result was agreed with the data sheet concluded from data base information for low phase Cu-1212 and high phase Cu-1223. The appearance of the two phase were accepted because we are talking about the polycrystalline phase. The XRD analysis was applied in the Refine program in order to find the lattice parameter $a=b=4.171 \text{ \AA}$ and $c=16.743 \text{ \AA}$. It was found that the Cu-1223 had a tetragonal phase, and the lattice constants were larger than the lattice parameter for Hg-1223 especially in the basal plane. That might be attributed to the more extra oxygen including in comparable to Hg-1223. The data-base of (ICDD) with pdf file (98-004-1652) [86] also, was used to analysis the pattern of Cu-1223 system. The small change in lattice constant might be related to the variation of (2θ) position. The observed change in lattice parameters were agreed with the strain happened in Cu-1223 compound that was (0.885 ± 0.149) .

The planes of low phase have a peaks (013), (005), (014), (015), (006), (022) and (025) with different intensity at $(2\theta=31.951, 35.349, 36.356, 42.758, 43.053, 49.761 \text{ and } 60.417)$ receptivity.

They were compared with the international center for diffraction data (ICDD) with pdf file (98-007-4104) [85], and the data concluded of Hg-1223 that was discussed before. I think that the principle planes increased in the Cu-1223 compound, which were the planes (006), (007), (008), (0010) at $(2\theta=34.153, 40.062, 58.178, \text{ and } 59.704)$ receptivity. The effect of full Cu-substitution might be appeared by the position of the principle planes. It was found the plane (006) had the same value of 2θ in Hg-1223. Where the plane (007) had a small shifting in (2θ) . On the other hand, the plane with (0010) was created in Cu-1223. The planes (110), (130) and (220) in Cu-1223 had the same effect of the plane (110) in Hg-1223 compound. They were linked the basal plane of the upper and the lower of unit cell. On the other hand, I think the plane

with hkl (020) was made to correlate the basal planes in the unit cell. It was indicated that the atoms of extra oxygen placed in the basal planes of the Cu-1223 unit cell. As well known, the mechanism of superconductivity is depending on the motion of the charge carrier through the principle planes along the a-c direction. That means the planes with hkl (022), (026), (027), (014), (016), (017), (0110) and (025) were considered the steps for the motion of charge carriers. There are two common peaks with hkl (115) and (111) of Hg-1223 and Cu-1223 compounds at a different intensity and a small shifting in (2θ).

The appearance of a new planes represented by (112), (117), (121), (123), (119) and (126) at ($2\theta = 34.855, 52.646, 54.045, 65.889, 64.453$ and 65.47) in Cu-1223. These planes act as a correlation factor between the principle planes along the c-axis. Increasing the concentration of these planes tend to increase the factors affected the mechanism of conductivity and then improve the T_c value. The decreasing in the intensity of all planes in Cu-1223 sample was attributed to the concentration of these planes in the unit cell. In general, the replacement of Hg ions by Cu ions was a positive factor in the process of linking between the layer within the unit cell. Then the enhancement of superconductivity mechanism was happened during the presence of Cu in the basal plane and forming the active bond (Cu_2O) that linking the basal plane.

The thing that was noticed the appearance of Cu-1223 phase like Hg-1223 with some variation in the lattice constant of the tetragonal unit cell. This result may be a positive effect in the resistivity measurement in order to determine the superconducting phase. There is a good agreement with the results done by Lokshine et al [67]. They prepared the superconductor compound ($\text{Hg}_{0.2}\text{Cu}_{0.8}\text{Ba}_2\text{Ca}_2\text{Cu}_3\text{O}_{8+\delta}$) by using sealed silica tubes. They found that the lattice parameters $a = b = 3.852 \text{ \AA}$ and $c = 15.793 \text{ \AA}$. The small difference in the crystal structure might be related to the appearance of the low phase Cu-

1212, which was formed by the ratio 26% of the whole structure. The result of the XRD analysis for the superconductor compound Cu-1223 show as in Fig. (3.3) where the sintering process repeated.

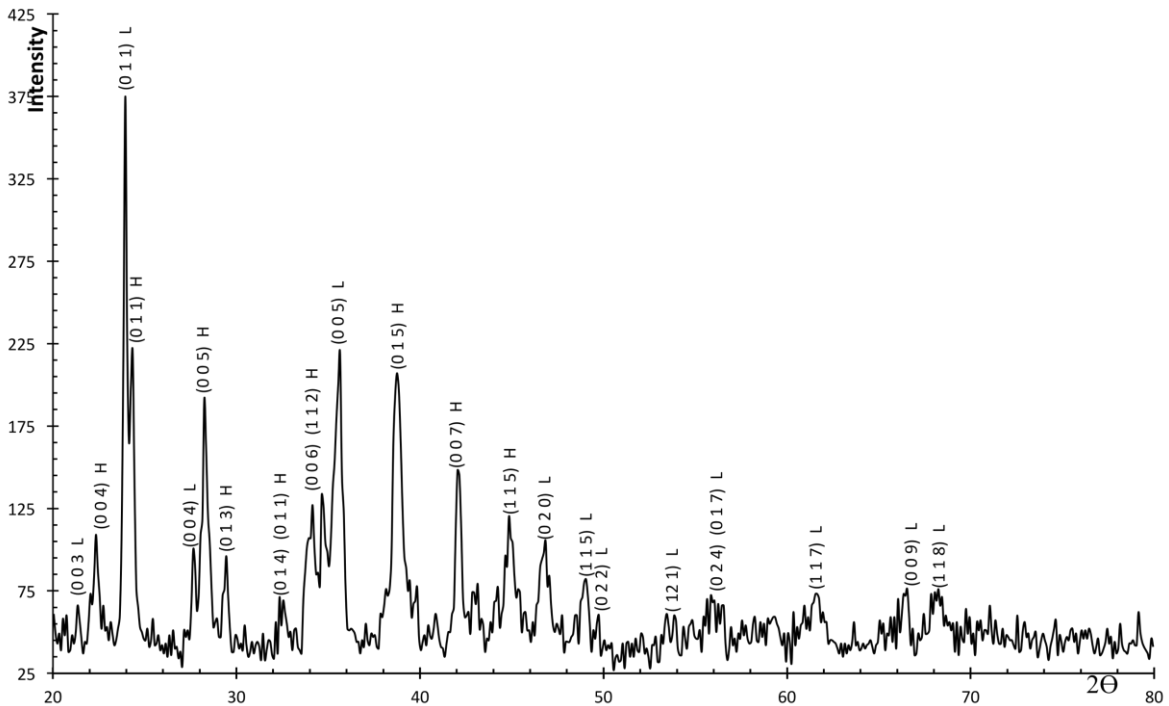


Figure (3.6); The XRD pattern for Cu-1212 compound.

It was found that the high phase Cu-1223 formalizes 45% of the whole structure and the low phase Cu-1212 formalize 54% of the whole structure, so the predominate phase is the low phase Cu-1212. On the other hand, the resistivity measurement, which will be discussed later, showed the low phase agreed with the result of XRD. The common peaks between the two last figure had the planes (005) and (022). The first plane has a small shifting in (2θ) and the second has the same position. Also, the common planes between the Hg-1223 and the second sintering of the Cu-1223 phase that had (003) at ($2\theta=21.361$) for Cu-1223 and (21.56) for Hg-1223. I think the planes (022), (011), (024) and (017) were represented the steps to satisfy the superconducting mechanism during the motion of charge carriers along the a-c direction through

the principle plane (005), (003), (004) and (009). It was observed that the appearance of the principle plane of Cu-1223 compound in second sintering sample less than in the first one. The plane (020) had played the same role in the high phase. It was linked the basal plane and check the symmetry of the structure. There was a new plane (118) occurred in the low phase. The applying of Refine program tend to conclude the lattice constant $a=b=3.55 \text{ \AA}$ and $c=12.37 \text{ \AA}$ as a tetragonal phase.

The results showed that there was a small different from the (ICDD) pdf number (98-007-4104) [85]. It might be related to the changing in 2θ position of the plane. They were agreed with the result of the strain in the Cu-1212 that (0.314 ± 0.194) . One can conclude that the increasing of the sintering time does not remove the low phase but the low phase predominated in the crystal structure for the sintered sample. In general, the carrier motion was directed in the a-c direction for Cu-1223 and Cu-1212 that was different from the Hg-1223 compound, the later was in b-c direction. The important thing was represented there was a negative effect by increasing the sintering time that showed the presence of low phase Cu-1212 rather than Cu-1221 as mentioned by Isawa et al. [84] but there was a difference in the period of sintering due to the difference in the phase Cu-1223.

The XRD pattern for the compound $(\text{SnBa}_2\text{Ca}_2\text{Cu}_3\text{O}_{8+0.2})$ which was completely substituted by Sn incomparable with the Hg-1223 compound as shown in Fig. (3.4). It was found that the presence of multi-phase, low phase Sn-1212 and high phase Sn-1223. Normally, there was a polycrystalline structure that showed the presence of two phases, that would be emphasized by the resistivity measurement. The application of refine program was suitable to find the lattice parameters for Sn-1223 phase $a=b=4.05 \text{ \AA}$ and $c= 15.682 \text{ \AA}$. There was increasing in the (a,b) parameters because the extra oxygen in Sn-compound was about (0.22). It was larger than the Hg-1223 phase, although the

atomic radius of Sn atom less than the atomic radius of Hg atom. On the other hand, there was decreasing in the c-parameter due to the polarized bond between Sn^{+2} and O^{-2} , and it was the same reason for the decreasing in (a,b) parameters for Sn in comparison with Cu-1223 phase. The polarized bond would be shifting the extra oxygen to take the interstitial site in the basal plane producing a pyramid-like shape.

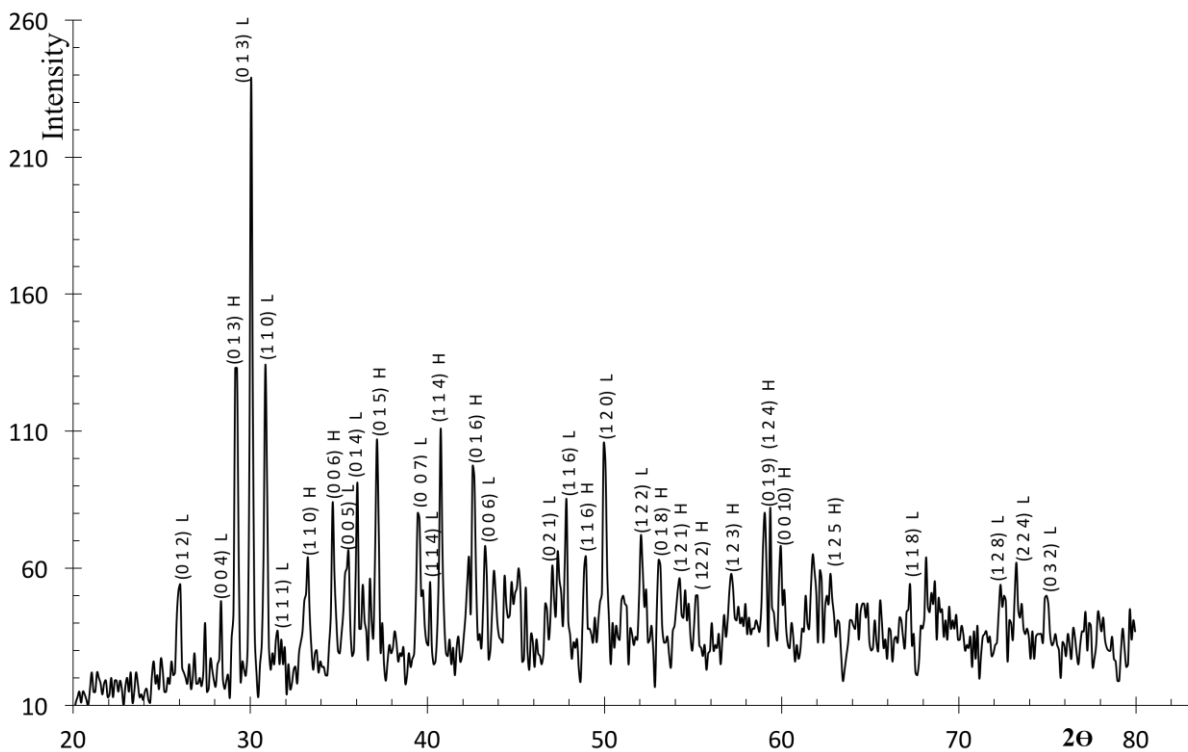


Figure (3.7); The XRD pattern for Sn-1223 compound.

The high phase of Sn-1223 has the plane (110) at ($2\theta = 33.269$) achieved the symmetry in the structure because it was linked the basal planes. There was a small shifting in (2θ) causing the change in the lattice parameters as mentioned in Hg-1223. The plane (006) might be considered active layer formed (O-O) bond. There was another plane (0010) was considered as an active layer in the mechanism of superconductivity. The common plane between Hg-1223 and Sn-1223 compound is (116) with the small shifting in (2θ) position that causing a changing in the lattice parameter. Whereas the planes (013), (015), (016), (018) and (019) might be considered as the steps for the charge carrier motion to

satisfy of the superconducting mechanism during the connection between the layers within the unit cell in (a-c) direction. This mechanism was similar to Cu-1223 compound and different from the Hg-1223 compound that was in (b-c) direction. There were many planes related to the high phase represented by (114), (121), (122), (123), (124) and (125). There was a common plane between two phases Cu-1223 and Sn-1223 represented by (016) with a small shifting in the position of (2θ). The common plane between Sn-1212 phase and Cu-1212 compounds represented by (005) with the small shifting in (2θ) that was considered one of the active layer. Another active layers represented by (004), (006) and (007).

There were a new planes created by (012), (013), (014), (021), (019) and (032) in Sn-1212 compound might be represented as the steps of the superconductivity mechanism through the active layer. Beside that there were another planes created by (114), (116), (120), (122), (118), (128), (224) and (032). The results showed that the (Sn-1223) compound had been analyzed by using the (ICDD) pdf number (98-004-1653) [86], (98-005-0262) [87], (98-0074135), (98-007-4136) [88] and (98-008-5327) [89]. We concluded that the full substitution by Sn in Hg-1223 was appeared a multi-phase Sn-1223 and Sn-1212). The changing in the lattice parameter that were agreed with the result of the strain for Sn-1223 ± 0.989 . The repeating of the sintering process had no effect on the results obtained because the compound ($\text{SnBa}_2\text{Ca}_2\text{Cu}_3\text{O}_{8+\delta}$) had two phase, the high and low phase normally. Table. (3-1) was given more details of crystal structure, Iodmetric titration and the correlation between them.

3.5 Resistivity measurement.

The resistivity measurement had been done for the samples under study to show the presence of high temperature superconductor for Hg-1223, Cu-1223, Cu-1212 and Sn-1223 compounds by using a cryogenic system of liquid helium as explained previously. The behavior of the resistivity versus temperature was

very important to define the metallic behavior for any materials under cooling state. It was considered an important technique to determine the critical temperature of the superconductor compound and then showed the superconductor behavior. The agreement of resistivity measurement results with XRD analysis was very important to show the required phase of the compound under study.

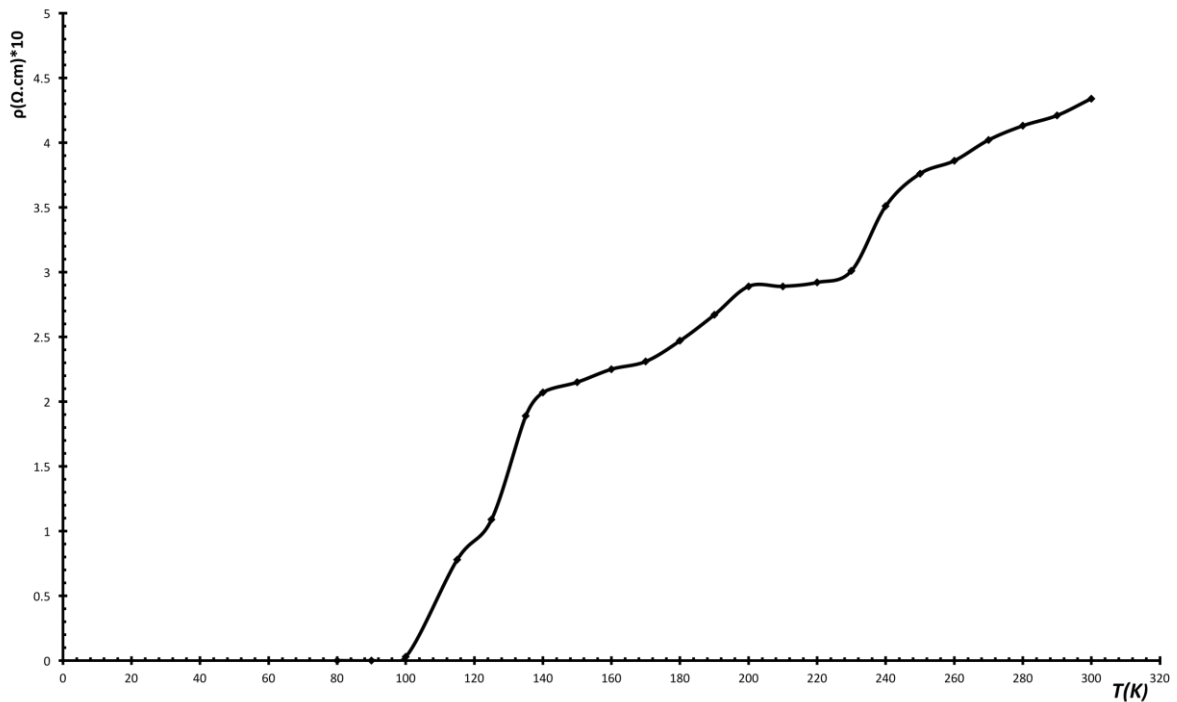


Figure (3.8); The electrical resistivity for Hg-1223 compound.

The electrical resistivity for the Hg-1223 has shown in Fig. (3.5). It was found that the normal resistivity for this compound was (1.2 Ωcm) with a critical temperature 115 K. Also, the $T_{Con} = 124$ K, $T_{Coff} = 104$ K and $\Delta T_c = 20$ K. The result showed the presence of high phase Hg-1223. It was emphasized by XRD analysis, which showed the predominate high phase of Hg-1223. The critical temperature was larger than 80 K that was related to high phase superconductor. Our results were approximately similar to Isawa et al. [84] they prepared the superconductor compound Hg-1223 by using encapsulation method. They found that the critical temperature of about 133 K. The behavior

of the resistivity was approximately similar with our behavior of resistivity. The difference between the results may be related to the condition of preparation and the appearance of the low phase Hg-1212 in the crystal structure in addition to high phase of Hg-1223. This is the reason why (T_c) is smaller than the T_c -value obtained by Isawa [84].

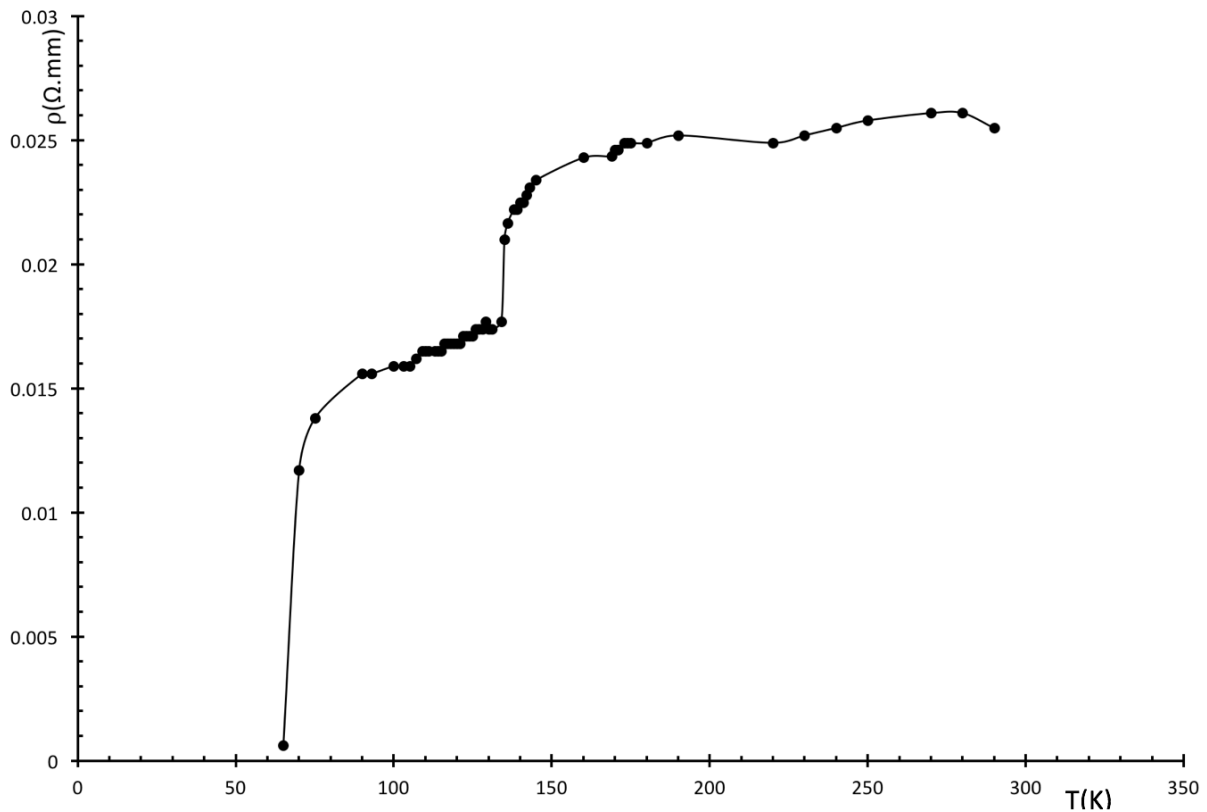


Figure (3.9); The electrical resistivity for Cu-1223 compound.

The electrical resistivity for Cu-1223 compound as a function of temperature is shown in Fig. (3.6). The behavior showed two regions in the resistivity curve, the first one was belong to the high phase of crystal structure and the second belong to the low phase. The high phase showed a normal resistivity of about (0.0215 $\Omega.mm$), critical temperature 128 K, $T_{C_{on}}$ 130 K, $T_{C_{off}}$ 127 K and ΔT_c 3 K. The low phase showed a normal resistivity of about (0.0115 $\Omega.mm$), T_c 66 K, $T_{C_{on}}$ 67 K, $T_{C_{off}}$ 64 K and ΔT_c 3 K. The appearance of two phases supported by the XRD results that showed the two phases Cu-1223

and Cu-1212 were present but the high phase Cu-1223 was predominated as mentioned before. It was found that the normal resistivity of Cu-1223 sample less than for Hg-1223 sample. The full substitution of Hg atoms by Cu atoms play an important role to decrease the normal resistivity. The T_c -value increased from 115 K in Hg-1223 to 128 K in Cu-1223 compound .

The thing was important in the energy gap related to coupling energy between the layer. On the other words, this energy was belonged to O-Cu-O layers. So, the increasing of this layer in Cu-1223 rather than Hg-1223 tend to increase the critical temperature. That was emphasized XRD result, where the conducting layers (006), (007) and (0010) in (Cu-1223) more than the conducting layer in Hg-1223. That might be increased the critical temperature in Cu-1223 compound. There is a good agreement with the results obtained by Lokshin et al. [67]. The replacement of Hg atoms by Cu atoms in the superconductor compound of Hg-1223 by using sealed silica tubes. They found that the superconductor compound ($Hg_{1-x}Cu_xBa_2Ca_2Cu_3O_{8+\delta}$) at $x = 0.8$ had the T_c -value of about 135 K. The small difference between their results and our results may be related to the same reason mentioned in the XRD result.

The electrical resistivity for the (Cu-1212) compound had been shown in Fig.(3.7). The attempt to get rid of the low phase that was occurred in (Cu-1223), it was necessary to repeat the sintering process. This process was tending to decrease the porous size and made the sample denser and then increase the normal conductivity. The result showed the appearance of low phase Cu-1212 was predominate in the crystal structure as emphasized by XRD results. The resistivity measurement supported a single phase represented by low phase. The critical temperature of Cu-1212 was occurred at 64 K, T_{con} 68 K, T_{coff} 62 K and ΔT_c 6 K. The normal resistivity of Cu-1212 compound (0.01 $\Omega \cdot mm$) which was less than the normal resistivity of Cu-1223 compound (0.0215 $\Omega \cdot mm$) due to the presence of single phase rather than Cu-1223. The decreasing of T_c -value

might be regarded to many reasons, the first one is related to the presence of single low phase. Secondary, the low phase of Cu-1212 means the conducting layers is smaller than the high phase of Cu-1223. As a result of that, the coupling between

the layers is very low intensity incomparable to high phase of Cu-1223.

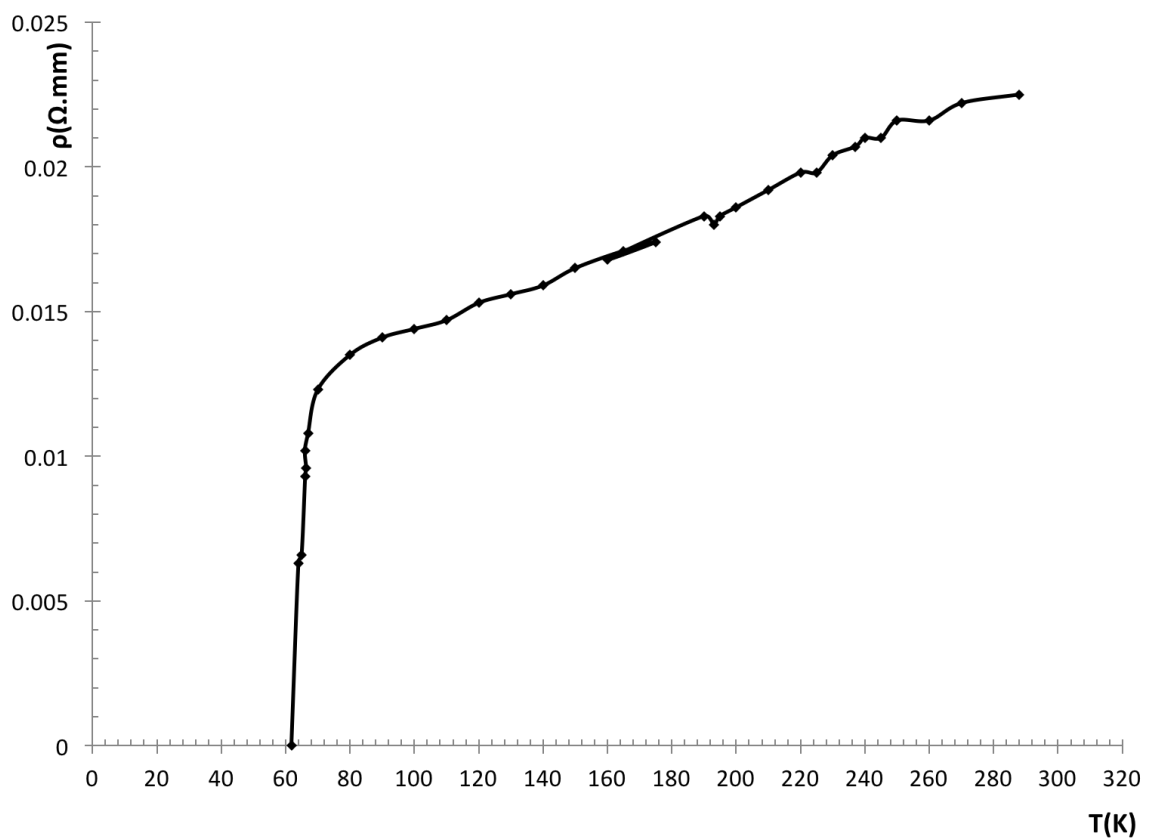


Figure (3.10); The electrical resistivity for Cu-1212 compound.

The electrical resistivity for Sn-1223 compound had been shown as in Fig. (3.8). This behavior showed that the drops occurred approximately at 133 K with normal resistivity (3.12 Ω.mm). The critical temperature of Sn-1223 compound was 110 K with T_{Con} 118 K, T_{Coff} 102 K and $\Delta T_c = 16$ K. In comparison with Cu-1223 sample it was founded that the normal resistivity of

Sn-1223 sample is more than the normal resistivity of Cu-1223 and less than the normal resistivity of Hg-1223 sample.

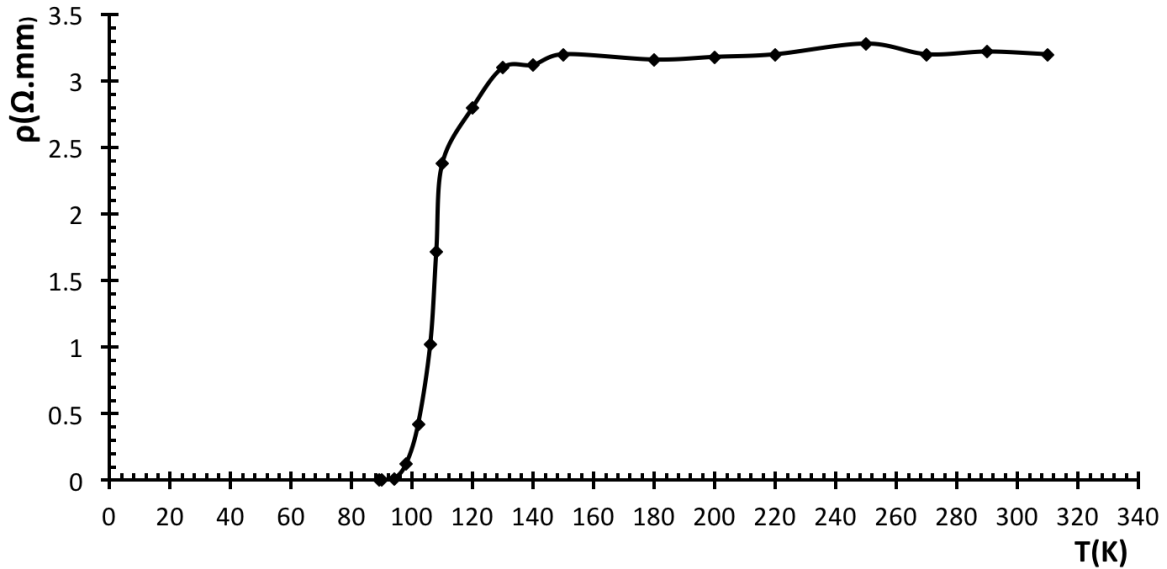


Figure (3.11); The electrical resistivity for Sn-1223 compound.

That was return to the concentration of charge carriers, which were responsible on the conductivity. The large conductivity means large concentration of charge carries and low conductivity means low charge carriers. On the other hand, the critical temperature of Sn-1223 compound was taking a value 110 K smaller than the values 115 K for Hg-1223 sample and 128 K for Cu-1223 sample.

On the other hand, the number of conductive layer is lower than the compound Cu-1223 and Hg-1223. The XRD result showed the presence of two phase, the low phase of Sn-1212 and high phase of Sn-1223. The high phase was predominated due to the resistivity result. The presence of low phase is another reason for decreasing the value of T_c . In general, the new families of Cu-1223 and Sn-1223 had a high- T_c superconducting state like to Hg-1223. The distinguishable thing in Cu-1223, Sn-1223 was the presence of low phase including the high phase. Whereas, Hg-1223 had just only high phase required.

Table.3-1 is indicating the value of (T_c) for all system dependent in this project correlated with the previous data obtained.

Table(3-1); Variation of lattice constant , δ - Value, Volume of Unit Cell, T_c -Value, for system with different samples (Hg-1223), (Cu-1223) and (Sn-1223).

Sample	δ - Value	Lattice Constant	Volume of Unit Cell (\AA^3)	T_c -Value	System
Hg-1223	0.07	a=b= 3.99 \AA , c= 16.47 \AA	262.20	115 K	Tetragonal
Cu-1223	0.1	a=b=4.17 \AA , c=16.74 \AA	291.09	128 K	Tetragonal
Cu-1212		a=b=3.55, c=12.37 \AA		64K	Tetragonal
Sn-1223	0.22	a=b=4.05 \AA , c=15.68 \AA	257.19	110 K	Tetragonal

3.6 Crystallite Size Measurement.

The samples were prepared by the solid state reaction examined by the XRD to find the lattice constant and the structural type by using the Refine program as mentioned before. The crystallite size and the non-uniform strain occurred in the crystal structure by using X-powder program during the Williamson-Hall method as shown in Fig. (3.9-12). The X-powder Williamson plots showed that the crystallite size for Hg-1223 compound was about (24.50 ± 3.05 nm) and the non-uniform strain (± 0.314) as appeared in Fig. (3.9). The

crystallite size for Cu-1223 compound had the value (10.77 ± 3.28 nm) and the non-uniform strain (0.885 ± 0.149) as shown in Fig. (3.10). The crystallite size for Cu-1212 compound was (13.56 ± 4.31 nm) and non-uniform strain was about (0.314 ± 0.194) as shown in Fig. (3.11). Finally, the crystallite size for Sn-1223 was about (13.50 ± 3.50 nm) and the non-uniform strain for Sn-1223 compound was about (± 0.989) as shown Fig. (3.12). Normally, the result of the non-uniform strain was supported the changing in the lattice parameters of the compounds. That might be returned to the nature of the bonds in the crystal structure, which are affected to the oxygen extra in the unit cell. The crystallite size of Cu-1223 was smaller than the crystallite size of Hg-1223 and Sn-1223. That was confirmed from the results of resistivity measurement that showed high T_c for Cu-1223.

Table (3-2); Crystallite size and non-uniform strain by using Williamson-Hall method for Hg-1223, Cu-1223, Cu-1212 and Sn-1223

Sample	Crystallite size by using Williamson-Hall method (nm)	Non-uniform strain
Hg-1223	24.5 ± 3.05 nm	± 0.314
Cu-1223	10.77 ± 3.28	0.885 ± 0.149
Cu-1212	13.56 ± 4.31	0.314 ± 0.194
Sn-1223	13.5 ± 3.5	± 0.989

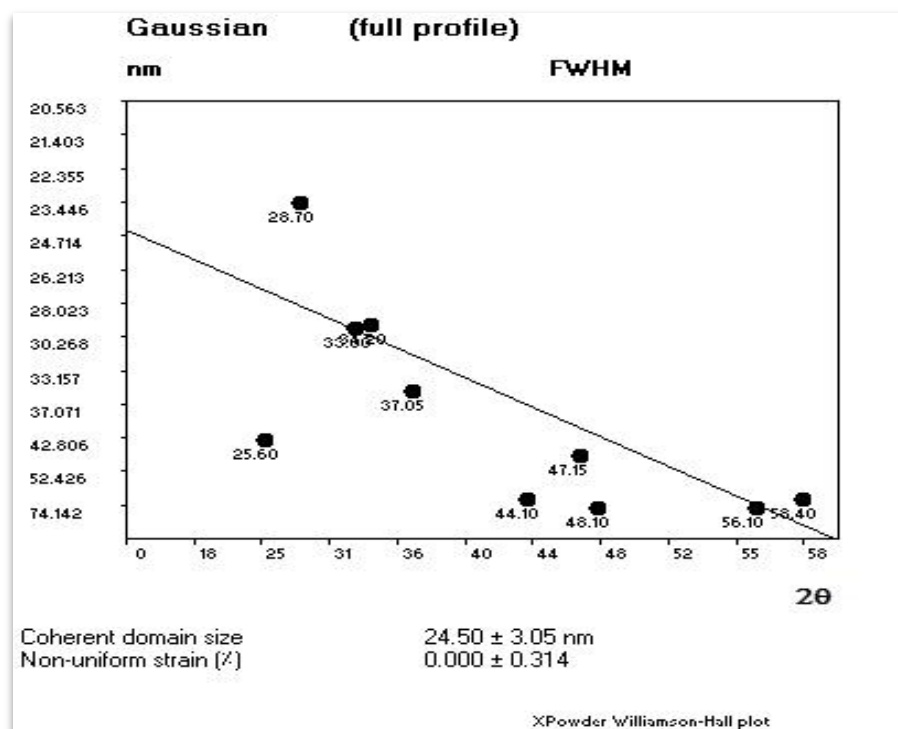


Figure (3.12); The crystallite size and the non-uniform strain for Hg-1223 compound.

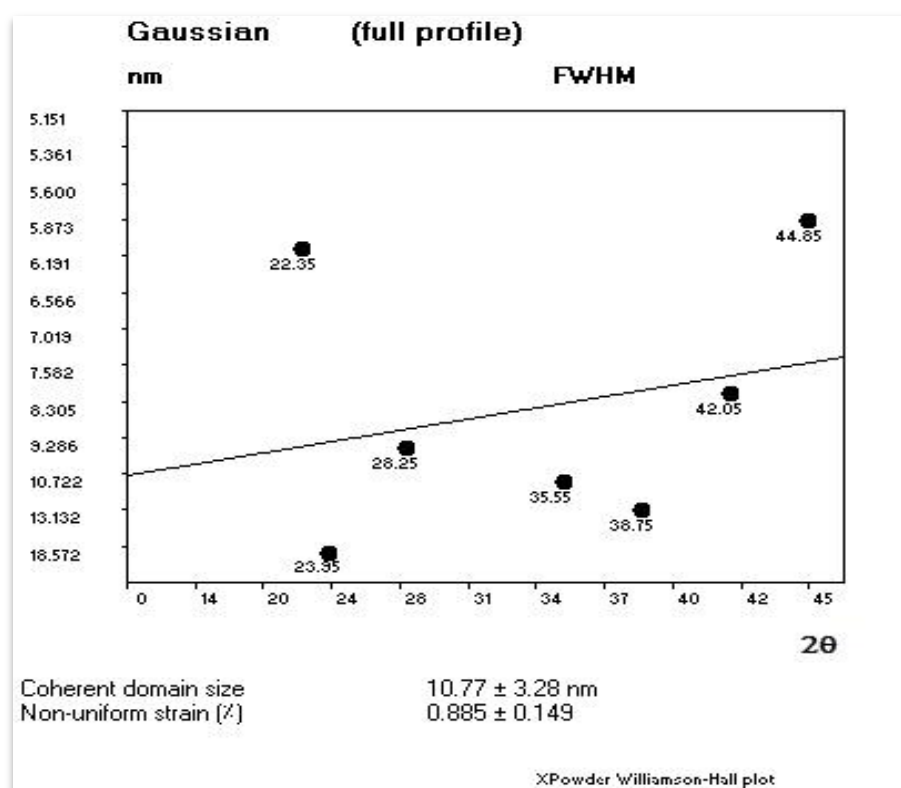


Figure (3.13); The crystallite size and the non-uniform strain for Cu-1223 compound.

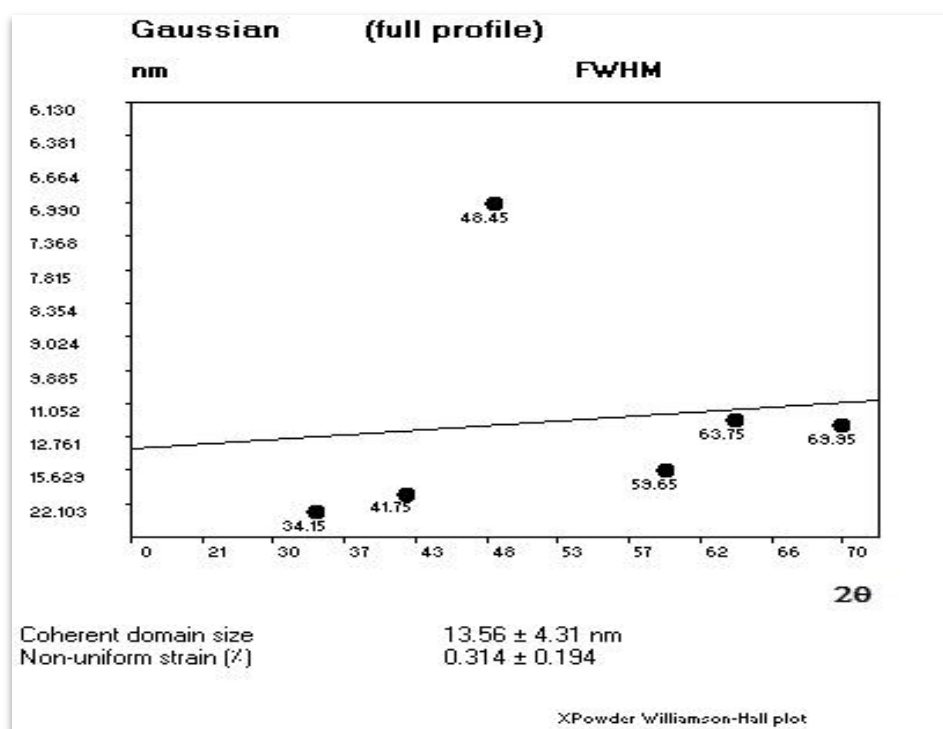


Figure (3.14); The crystallite size and the non-uniform strain for Cu-1212 compound.

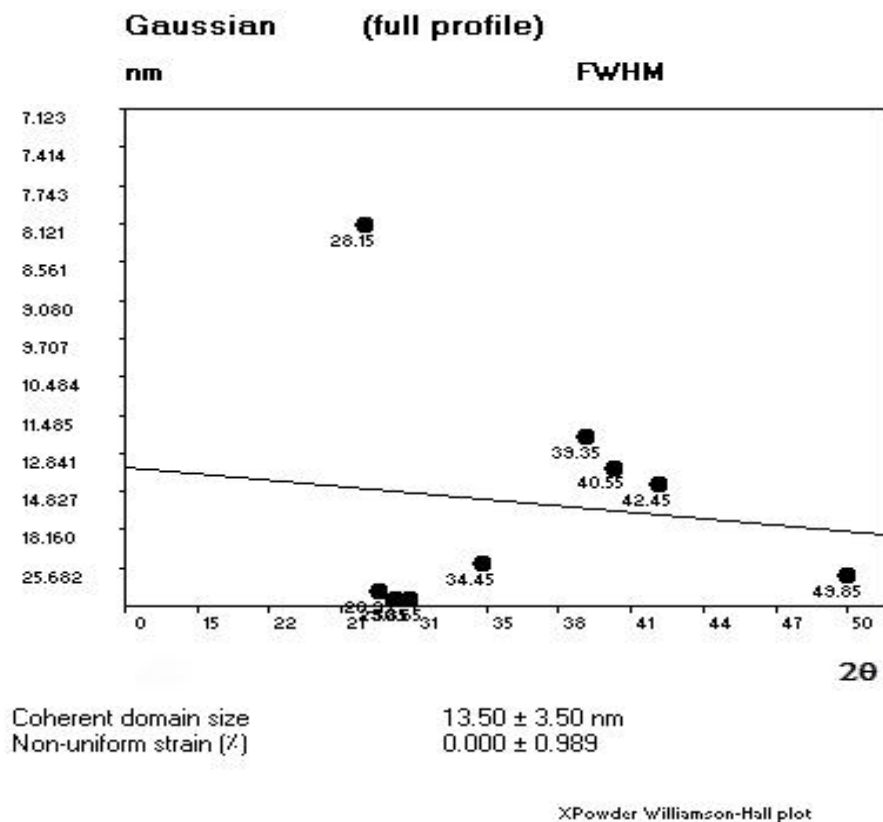


Figure (3.15); The crystallite size and the non-uniform strain for Sn-1223 compound.

3.7 Scanning Electron Microscope (SEM) Result.

The analysis of SEM was another important technique beside the whole previous results to complete the full specification of the samples under study. The information of the porous, homogeneity occurred in the structure and the grain size. The SEM-photos for Hg-1223, Cu-1223, and Sn-1223 superconductor compounds had been shown as in Fig. (3.16-18) respectively. The photos exhibited that the grain size for Hg-1223 sample ranging between ($1.2 \mu\text{m}$ - $3.1 \mu\text{m}$), for Cu-1223 sample ($1 \mu\text{m}$ - $3 \mu\text{m}$) and for Sn-1223 sample ($1.6 \mu\text{m}$ - $5.4 \mu\text{m}$). The small range of grain size for Cu-1223 was indicated to the small porous size that had direct effect on decreasing the scattering factor. That was emphasized by smaller the normal resistivity as discussed before. The large grain size for Sn-1223 was the reason for the large resistivity as mentioned from resistivity measurement as discussed before.

It was clear that the convergence in the grain size tend to a good indication for the homogeneity in the crystal structure for all compounds beside the effect of the grinding during the synthesis process. It was observed that the porous between the grains was decreased by replacement of Hg by Cu and Sn atoms and forming a new family related to Hg-1223. The increasing of the porous would effect on the physical properties of the sample by increasing the scattering factor and then decreasing the normal conductivity. On the other hand, the porous concentration depends on two factors represented by the sintering time and the pressing. This technique was a complement one to specify the new high- T_c superconducting phase like Cu-1223 and Sn-1223 rather than the phase Hg-1223.

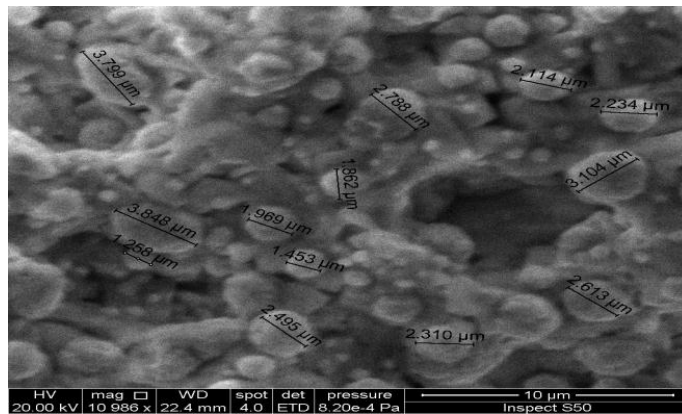


Figure (3.16); The SEM for Hg-1223 superconductor compound.

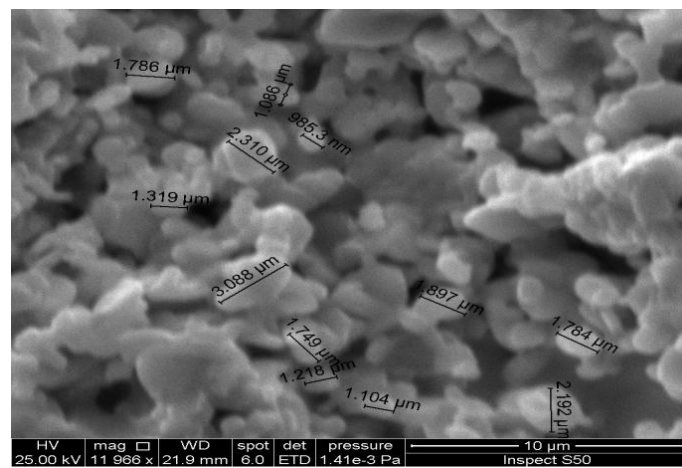


Figure (3.17); The SEM for Cu-1223 superconductor compound.

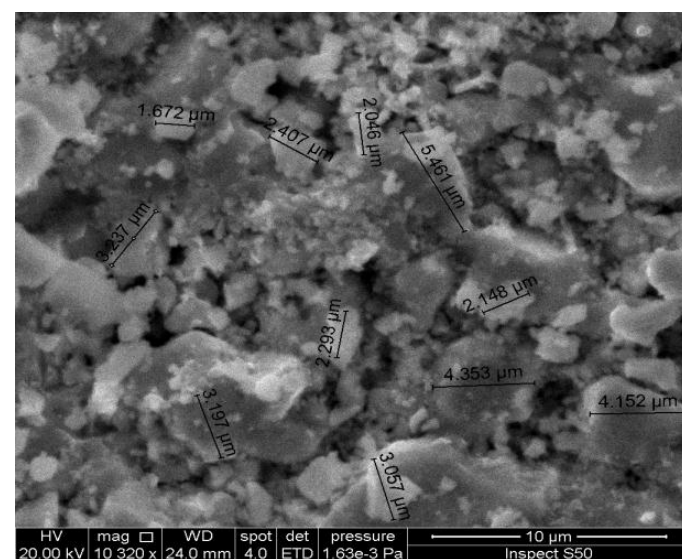


Figure (3.18); The SEM for Sn-1223 superconductor compound.

Chapter Four

Conclusion and Future Work

4.1 Conclusion

We can conclude from our results as follow.

- 1- The synthesis of the superconductor compound $HgBa_2Ca_2Cu_3O_{8+\delta}$ Hg-1223 is possible under special condition by using evacuated sealed quartz tube at 850 °C for 10 hr. , Where $T_c = 115K$.
- 2- The Hg atoms could be full substituted by Cu and Sn atoms to form the novel superconductor compounds $CuBa_2Ca_2Cu_3O_{8+\delta}$ Cu-1223 and $SnBa_2Ca_2Cu_3O_{8+\delta}$ Sn-1223 with a critical temperature $T_c= 128 K$ and 110 K receptively.
- 3- As a result, repeating of the sintering process to get ride of Cu-1212 phase in the HTSC Cu-1223 phase, the low phase Cu-1212 predominated in the crystal structure with $T_c=64 K$.
- 4- The main conclusion is related to the formation of new high- T_c superconducting families like Cu-1223 and Sn-1223 on the style of Hg-1223. Both new families obtained are including the high and low phases with in the polycrystalline behavior of the samples under study. This is considered very important point because many universities and institutes in global searching to find a new high- T_c approach to room temperature.

4.2 The future works

- 1- It will be possible to prepare the samples mentioned previously by sol-gel technique to get more details about them.
- 2- Using the hydrothermal technique to prepare these new families Cu-1223 and Sn-1223, and studying its properties.

- 3- The above two points may be producing the nanostructure. It is necessary to search on the preparation of nanostructure of Cu-1223 and Sn-1223.
- 4- The preparation of flexible wire of the new compounds of Cu-1223 and Sn-1223 and studying it is industrial applications.
- 5- Studying the effect of the raw materials grain size on the physical properties of the prepared superconducting samples.

References

- [1] W.Bucked, R.Kleiner, “Superconductivity – Fundamentals and Applications” , Wiley-VCH Verlag, Weinheim (2004).
- [2] Md.Atikur Rahman, Md.Zahidur Rahamau and Md.Nurush Samsuddoha, “A Review on Cuprate Based Superconducting Materials Including Characteristics and Applications”, American Journal of Physics and Applications, 3 (2), PP. 39-56, (2015)
- [3] Shoji Tanaka, “High-Temperature Superconducting”, Jpn. J. Appl. Phys., 45 (12), (2006).
- [4] A.S.Alexandrov, “Theory of Superconducting Form Weak to Strong Coupling”, IOP Publishing Ltd, UK University, (2003).
- [5] W.Meissner and R.Oschenfeld , “Ein Neuer Effekt Bei Eintritt Der Supraleitfähigkeit”, Naturwissenschaften, .21(44), PP.787-788, (1933).
- [6] V.L.Ginzburg and L.D.Landau, “on The Theory of Superconductivity”, Zh.Ekps.Teor.Fiz, 20, 1064, (1950).
- [7] E.Maxwell, “Isotope Effect in The Superconductivity of Mercury”, Phys.Rev, 78, 477, (1950).
- [8] J.Bardeen,L.N.Cooper and J.R.Schieffer, “Theory of Superconductivity”, phys.Rev.108,1175,(1957).
- [9] J.E Kunzler, E.Buehler, F.S.L.Hsu and J.H Wernick, “ Superconductivity in Nb_3Sn at High Current Density in a Magnetic Field of 88 Kgauss”, Phys, Rev.Lett.6 (89), (1961).
- [10] T.G.Berlincourt and R.R.Hake, “Pulsed Magnetic Field Studies of Superconducting Transition Metal Alloys at High and Low Current Densities”, Bull. Am.Phy.Soc.II7, 408, (1962).
- [11] T.G Berlincourt, “Emergence of Nb-Ti as Super Magnet Material Cryogenics”, 27, 283, (1987).

- [12] B.D. Josephson, "Possible New Effect in Superconductivity Tunneling", *Phy. Lett*, 1(7), PP. 251-253, (1962).
- [13] J.G Bednorz and K.A.Mueller, "Possible High T_c Superconductivity in The Ba-La-Cu-O", *Z.Phys.B*, 64(2), PP.189-193, (1986).
- [14] M.K Wu, J.R.Ashbarn, C.J.Torng, P.H. Hor, R.L.Meng, L.Gao, Z.J.Huang, Y.Q.Wang and C.W.Chu, "Superconductivity at 93K in a New Mixed-Phase Y-Ba-Cu-O Compound System at Ambient Pressure", *Phys. Rev. Lett*, 58, 908, (1987).
- [15] H.Maeda, Y.Tanako, M.Fukutomi and T.Asano, *Jap.J.Appl.* "A New High- T_c Oxide Superconductor Without a Rare Earth Element", *Phys.*, 27(2),pp. L209-L210, (1988).
- [16] A.Schilling, M.Gantani, J.D.Guo and H.R.Ott, "Superconductivity Above 130K in Hg-Ba-Ca-Cu-O", *Nature*, 56, 363, (1993).
- [17] Cw Chu, L Gao, F.Chen, Z.J.Huang, Rl.Meng and Yy Xue, "Superconductivity above 150 K in $HgBa_2Ca_2Cu_3O_{8+\delta}$ at High Pressures", *Nature*, 365, PP. 323-325, (1993).
- [18] N.Khare, "Handbook of High-Temperature Superconductor Electronics", Marcel Dekker, (2003).
- [19] M.R.Beasley, "A History of Superconductivity", Edited by K.Ishiguro (EDS), "Advances in Superconductivity", Proceeding 1st International Symposium on Superconductivity (ISS88), Nagoya, 3(1988).
- [20] A.I. Hamodi, "The Effect of Parameters (n) on Superconducting Properties of $MNCa_{n-1}Cu_nO_x$ $M = (Hg, Bi_2)$, $N = (Ba_2, Sr_2)$ ", M.Sc. Thesis, Al-Nahrain University, College of Science, (2013).
- [21] Dh wu, S.Sridhar, Dong-Ho Wu and S.Sridhar, "Pining Forces and Lower Critical Fields in $YBa_2Cu_3O_y$ Crystals : Temperature Dependence and Anisotropy", *Phys.Rev.Lett*.66, 968 (1991).
- [22] L.Solymar and D.Walsh, "Electrical Properties of Materials", Oxford University Press, Ch.14, (1998).

- [23] P.Chaudhari, J.Mannhart, D.Dimos , CC Tsuei , Jchi.Mm Oprysko and M.Scheuermann, “Direct Measurement of the Superconductor Properties of Single Grain Boundaries in $Y_1Ba_2Cu_3O_{7-\delta}$ ”, Phys. Rev. Lett. 60, PP. 1653-1656, (1988)
- [24] Ak.Gupta, Sk.Agarwal, B.Jayaram , A.Gupta and Av.Nurlikar, “Observation of Invers ac Josephson Effect in Bulk Y-Ba-Cu-O Possessing high T_c ”, J.Phys., Parmena, 28, PP.L705-L707, (1987).
- [25] H.P. Myers, “Introducing Solid State Physics”, (1990).
- [26] J.W.Garland, “Isotope Effect in Superconductivity”, Phys, Rev. Lett 11, 114, (1963).
- [27] A.A.Abrikosov, “On The Magnetic Properties, of Superconductor of The Second Group”, Soviet Phys., JETP, 5, PP.1174-1182, (1957).
- [28] M.A.Omar, “Introducing to Solid State Physics” , Addison Wesly Publshing Company, London, (1974).
- [29] Z.Tesanovic, “Role of Inter Layer Coupling in Oxide Superconductor“, Edited by J.Halley ”Theory of High Temperature Superconductor“, Addison-Wesly Publishing Company, New York, (1988) .
- [30] M.Crisan, “Theory of Superconductivity“, World scientific co Pte Ltd, Singapore, (1989).
- [31] J.R.Gavaler, “Superconductivity in Nb-Ge Films above 22K”, Appl.Phys.Lett, 23, 480, (1973).
- [32] C.P.Poole, H.A.Farach and R.J.Creswick (EDS), “Superconductivity”, Academic Press, California, (1995).
- [33] Cw.Chu, PH.Hor, RL.Meng , L.Gao and ZJ.Huang, “Superconductivity at 52.5K in the Lanthanum-Barium-Copper-Oxide System”, Science 235,PP. 567-569, (1987).
- [34] RJ.Cava , B.Batlogy ,RB.Vancouver , DW.Murphy , S.Sunshine ,T.Siegrist, JP Re-Meika, Ea.Rietman, SZhurak and Gp.Espinosa, “Bulk Superconductivity

- at 91K in Single Phase Oxygen-Deficient Perovskite $Ba_2YCu_3O_{9-\delta}$ ”, Phys. Rev Lett. 58, PP.1676-1679, (1987).
- [35] RM.Hazen, Lw.Finger, Rj.Angel, Gj.Prewitt, NL.Ross, HK.Mao, CG.Hadidacos, PH.Hor, RL.Meng and CW.Chu. “Crystallographic Description of Phases in the Y-Ba-Cu-O Superconductor”, Phys. Rev.B35, PP. 7238-7241, (1987).
- [36] CNR.Rao, P.Ganguly, AK.Raychaudhuri, Ram.Ram, K.Seedhar, “Identification of Phase Responsible for High-Temperature Superconductivity in YBa Cu Oxide”, Nature, 320, PP.856-857, (1987).
- [37] Z.Z.Sheng and A.M.Hermann, “Bulk Superconductivity at 120K in the T-Ca/Ba-CuO System”, Nature, 332, PP.138-139, (1988).
- [38] SN.Putillin, EV.Anti Pov, O.Chmaissem and M.Marezio, “Superconductivity at 94K in $HgBa_2CuO_{4+\delta}$ ”, Nature, 362, PP.226-228, (1993).
- [39] L.Gao et al., ”Superconductivity up to 164K in $HgBa_2Ca_{m-1}Cu_mO_{2m+2+\delta}$ (m=1,2,3) Under Quasihydrostatic Pressures”, Phys. Rev., 50(6), PP.4260-4263, (1994).
- [40] A.Mourachkine, “Room Temperature Superconductivity”. Cambridge International Science Publishing, P.310, (2004).
- [41] Ajay,”Role Of Interlayer Coupling In The Superconducting State Of Layered Cuprate Superconductors”, 316(3), PP.267-272, 20 May (1999).
- [42] P. Dai," B.C. Chakoumakos, G.F. Sun, K.W. Wong, Y. Xin and D.F. Lu, “Synthesis and Neutron Powder Diffraction Study Of The Superconductor $HgBa_2Ca_2Cu_3O_{8+\delta}$ By Tl Substitution ", Physica C, 243, PP. 201-206 ,(1995).
- [43] A. Maignan, D. Pelloquin, M. Hervieu, C. Michel and B. Raveau, “New Superconducting Vanadomercury Cuprates $Hg_{0.8}V_{0.2}Ba_2Ca_{m-1}Cu_mO_{2m+m+\delta}$ ”, Physica C, 243, PP.214-22, (1995).
- [44] Xiao-Gang Wang, Z. Huang and L. Yuan, “Effect of F-Doping in The Hg-Ba-Ca-Cu-O System”, Physica C, 253, PP. 254-258,(1995).

- [45] W.L. Lechter, L.E. Toth, M.S. Osofsky, E.F. Skelton, A.R. Drews, C.C. Kim, B. Das, S.B. Qadri, A.W. Webb and R.J. Soulen Jr, "Superconductivity in (Hg,Tl)(Ba,Sr)CaCuO_x", *Physica C*, 242, PP.221-227, (1995).
- [46] G.V. Tendeloo, M. Hervieu, X.F. Zhang and B. Raveau, "Ordering Principles and Defect Structure of "1201", "1212", and "1222" Type (Hg,Pr)-Sr-(Sr,Ca,Pr)-Cu-O Superconductors", *Journal of Solid State Chemistry*, 114, PP.369-378, (1995).
- [47] J.H. Du, H.M. Shao, Q. Li, D. Feng and G.J. She, "TEM Study of Pb-Doped Hg-Ba-Ca-Cu-O Superconductor", *Solid State Communication*, 99(11), PP.863-867, (1996).
- [48] X. Chen, Z. Xu, J. Wang, Z. Jiao and Q. Zhang, "Oxidation State of Copper and Superconductivity in The Hg-Ba-Ca-Cu-O System", *Chemical Phys. Lett.*, 258, PP.1-5, (1996).
- [49] J. B. Mandal, B. Bandyopadhyay, F. Fauth, T. Chattopadhyay and B. Ghosh, "a New Mercury-Based High- T_c Cuprate $Hg_{0.7}V_{0.3}Sr_{2-x}La_xCuO_{4+\delta}$ ", *Physica C*, 264, PP.145-153, (1996).
- [50] T. Tatsuki, A. Tokiwa-Yamamoto, T. Tamura, X.J. Wu, Y. Moriwaki, S. Adachi and K. Tanabe, "Structural and Superconducting Properties of $(Hg_{1-x}Tl_x)_2Ba_2Ca_{n-1}Cu_nO_y$ (n=3,4) Superconductors Prepared Under High Pressure", *Physica C*, 273, PP. 65-71, (1996).
- [51] Y.S. Yao, W. Liu, Y.J. Su, Y.F. Xiong, W.J. Ma, G.H. Cao, G.T. Zou and Z.X. Zhao, "New Phase of Hg-2435 in the Hg-Ba-Ca-Cu-O Oxide System", *Physica C*, 282-287, PP.897-898, (1997).
- [52] J.L Tholece, P. Toulemonde, A. Sulpice, C. Acha, M. Nunez-Regueiro, J.J. Capponi, C. Chailout, M. Alario-Franco, E. Gautier, S. Le Floch, M. Marezio, P. Bordet, S.M. Loureiro, S.N. Putilin and E.V. Antipov, "Superconducting Properties of The Mercury and Cu/C Phase", *Physica C*, 282-287, PP.857-858, (1997).

- [53] O. Chmaissem, J.D. Jorgensen, D.G. Hinks, B.G. Storey, B. Dabrowski, H. Zhang and L.D. Marks, "Structure And Superconductivity In Cr-Substituted $HgBa_2CuO_{4+\delta}$ ", *Physica C*, 279, PP.1-10, (1997).
- [54] E.V. Antipov, S.N. Putilin, R.V. Shanchenko, V.A. Alyoshin, M.G. Rozova, A.M. Abakumov, D.A. Mikhailova, A.M. Balagurov, O. Lebebev and G. Van Tendeloo, "Structural Features, Oxygen and Fluorine Doping in Cu-based Superconductores", *Physica C*, 282-287, PP.61-64, (1997).
- [55] J. Karpinski, H. Schwer, E. Kopnin, R. Molinski, G.I. Meijer and K. Conder, "High Gas Pressure Crystal Growth and Properties of $HgBa_2Ca_{n-1}Cu_nO_{2n+2+\delta}$, $Sr_{0.73}CuO_2$ and $Ca_xA_{1-x}CuO_2$ " *Physica C*, 282-287, PP.77-80, (1997).
- [56] P.V.P.S.S. Sastry, K.M. Amm, D.C. Knoll, S.C. Peterson and J. Schwartz, "Synthesis and Processing of Bi-Doped $Hg_1Ba_2Ca_2Cu_3O_y$ Superconductors", *Physica C*, 300, PP.125-140, (1998).
- [57] K.A Lokshin , D.A. Pavlov, M.L. Kovba, E.V. Antipov, I.G. Kuzemskaya, L.F. Kulikova, V.V. Davydov, I.V. Morozov and E.S. Itskevich, "Synthesis and Characterization of Overdoped Hg-1234 and Hg-1245 Phases; The Universal Behavior of T_c Variation in The $HgBa_2Ca_{n-1}Cu_nO_{2n+2+\delta}$ Series", *Physica C*, 300, PP.71-76, (1998)
- [58] A.K.Pandey, G.D.Verma and O.N. Srivastava, "Investigation on The Tl-Doped Hg-Ba-Ca-Cu-O High Temperature Superconductor in Regard to Hole Doping and Microstructure Characteristics", *Physica C*, 306, PP.47-57, (1998).
- [59] C. Acha, M. Nunez-Regueiro, S. Le Floch, P. Bordet, J.J. Capponi, C. Chailout and J-L Tholence, "Overdoped $Hg_{1-x}Au_xBa_2Ca_2Cu_3O_{8+x}$ and The Origin of The Intrinsic Increase of T_c Under Pressure in Mercury Cuprates", *The American Physical Society*, 57(10), PP.5630-5633, (1998).
- [60] S.S Yom, Jong-Ku Park, G.H. Kim, H.S. Kim, J.Y. Lee, E.S. Ghoi and Y.W. Park, "Resistivity Anomalies at Near 250k in Hg-Ca-Cu-O and Fe-S

- Systems", International Journal Of Modern Physics, 13(29,30,31), PP.3755-3757, (1999).
- [61] M. Valldor, I. Bryntse and A. Morawski, "Synthesis and X-ray Single-Crystal Analysis of a 2212-type Superconductor in The Tl-Hg-Sr-Ca-Cu-O System", Physica C, 314, PP. 27-35, (1999).
- [62] MTD Orlando, A.G Cunha, S.L. Budko, A. Sin, L.G. Martinez, W. Vanoni, H. Belich, X. Obradors, F.G. Emmerich and E. Baggio-Saitovitch, " $Hg_{0.95}Re_{0.05}Ba_2Ca_2Cu_3O_{8+\delta}$ Superconductor: Sample Preparation and Transport Properties Under HydroStatic Pressure", Supercond. Sci. Technol., UK, 13, PP.140-147, (2000).
- [63] D.C Kim, J.S. Kim, S.J. Joo, H.R. Kang and Y.W. Park, "Synthesis and Electrical Transport of $Hg_{0.8}Tl_{0.2}Ba_2Ca_2Cu_3O_{8+\delta}$ ", Physica C, 341-348, PP.1907-1908, (2000).
- [64] G. Celotti, A. Tampieri and F. Monteverde, "A New Cu-Free Cubic Phase as Competitor in The Synthesis of Hg(Re)-1223 Superconductor", Solid State Communications, 116, PP.109-114, (2000).
- [65] D. Sedmidubsky, J. Leitner, K. Knizek, A. Strejc and M. Nevriava, "Phase Relations in Hg-Ba-Ca-Cu-O Systems", Physica C, 341-348, PP.509-510, (2000).
- [66] R.Giri, H.K.Sinch, R.S.Tiware and O.N.Srivastava, "Effect of Cationic Size in $Hg(Tl/Bi)Ba_2Ca_2Cu_3O_{8+\delta}$ on Superconducting and Microstructure Characteristics", Bull. Mater. Sci, 24(5), PP.523-528, (2001).
- [67] K.A. Lokshin, D.A. Pavlov, M.L. Kovba, S.N. Putilin, E.V. Antipov and I. Bryntse, "Synthesis and Investigation of $(Hg_{1-x}Cu_x)Ba_2Ca_2Cu_3O_{8+\delta}$ ", Physica C, 366, PP. 263-269, (2002).
- [68] A.J. Batista-Leyva, M.T.D.Orlando, L. Rivero, R. Cobas and E. Altshuler, "The Resistive Transition of $(Hg_{0.85}Re_{0.15})(Ba_{1-y}Sr_y)_2Ca_2Cu_3O_{8+\delta}$ Superconducting Polycrystals", Physica C, 383, PP.365-373, (2003).

- [69] E. Kandyel, "Synthesis, Structural and Physical Properties of New Terbium Containing Tb-Hg-Sr-Ca-Cu-O Superconducting System", *Journal of Physics and Chemistry of Solid*, 64, PP. 731-739, (2003)
- [70] R. Giri et al., "Investigations On the Synthesis And Microstructural Characteristics of Hg(Bi)-Ba-Ca-Cu-O HTSC in Relation to Critical Current Dersity", *Joural of Alloys And Compounds* 366, 254-263, (2004).
- [71] M.Zehetmayer, M.Eisterer. S.M.Kazakov, J.Karpinski, A.Wisniewski, R.Puzniak, A.Daignere and H.W.Weber, "Effect of Neutron and Electron Irradiation on Superconducting $HgBa_2CuO_{4+\delta}$ Single Crystals", *Physica C*, 408-410, PP. 30-31, (2004).
- [72] Elsayed Kandyel, "Synthesis, Structural and Transport Properties of (Hg,Fe)-1212 Superconducting Cuprate", *Physica C*, 422, PP. 102-111, (2005).
- [73] R.Corsini, A.D.Bortolozo, M.S da Luz, R.Ricardo da Silva, C.A.M. dos Santos and A.J.S. Machado, "Superconductivity in a New Quaternary Phase With $HgSm_{0.5}In_{0.5}Pb_2$ Composition", *Materials Letters* ,(2006).
- [74] M.T.D.Orlando, C.A.C.Passos, J.L.Passamai Jr, E.F.Medeiros, C.G.P.Orlando, R.V.Sampaio, H.S.P.Correa, F.C.L.de Melo, L.G.Martinez and J.L.Rossi, "Distortion of ReO_6 octahedron in The $Hg_{0.82}Re_{0.18}Ba_2Ca_2Cu_3O_{8+d}$ Superconductor", *Physica C*, 434, PP. 53-61, (2006).
- [75] C.A.C.Passos, J.L.Passamai.Jr, M.T.D.Orlando, E.F.Medeiros, R.V.Sampaio, F.D.C.Oliveira, J.F.Fardin and D.S.L.Simonetti, "Application of The (Hg,Re)-1223 Ceramic on Superconducting Fault Current Limiter", *Physica C*, 460-462, PP. 1451-1452, (2007)
- [76] M.F.Alias, G.Y.Hermiz, A.F.Abdul-Ameer and L.K.Abbas, "Effect of In Substitution on T_C and Superconducting properties of the $Hg_{1-x}In_xBa_{2-y}Sr_yCa_2Cu_3O_{8+\delta}$ ", *Proceeding of 3rd Scientific Conference*, PP.2259-2269, (2009).

- [77] O.Babych, Ya.Boyko, I.Gabriel, R.Lutciv, M.Matviyiv and M.Vasyuk, "Preparation and properties of Doped Hg-Based Superconducting Copper Oxides", *Acta Physica Polonica A*, 117, (2010).
- [78] T.M.Mendonca, P.B.Tavares, J.G.Correia, A.M.L.Lopes, C.Darie and J.P.Araujo, "The Urea Combustion Method in The Preparation of Precursors for High- T_c single phase $HgBa_2Ca_2Cu_3O_{8+\delta}$ superconductor", *Physica C*, 471, 1643, (2011).
- [79] Akram R.Jabur, " $Bi_{2-x}Hg_xSr_{2-y}Ba_yCa_2Cu_2O_{10}/Ag$ Sheath HTSC Wires, (Hg,Ba) Substitution Effect on The Critical Temperature", *Energy Procedia*, 36, PP. 985-994, (2013).
- [80] H. Ehrenreich and D. Turnbull, "solid state physics", Academic Press, 24, (1989).
- [81] K.S.Ghandhi, "Theory And Practice Of Microelectronics", Edited By John Willy And Sons,(1968).
- [82] A.Manthiran, J.S.Swinnea, Z.T.Sui, H.Steinfink and J.B.Goodenough, "The Influence of Oxygen Variation on The Crystal Structure And Phase Composition of The Superconductor Yttrium Barium Cooper Oxide $YBa_2Cu_3O_{7-x}$ ", 109, 22, 6667,(1987).
- [83] D.Mcmullan, "Scanning electron Microscopy 1928-1965",17(3), PP.175-185, (1995).
- [84] K.Isawa, A.Tokiwa-Yamamoto, M.Itoh, S.Adachi and H.Yamauchi, "Encapsulation Method for The Synthesis of Nearly Single-Phase Superconducting $HgBa_2Ca_2Cu_3O_{8+\delta}$ With $T_c \geq 135K$ ", *Physica C*, 222, PP.33-37, (1994).
- [85] D.G.Hinks, J.D.Jorgensen, G.S.Knapp, M,A.Beno, B.A.Hunter, J.L.Wagner and P.G.Radaelli, "Structure, Doping and Superconductivity in $HgBa_2CaCu_2O_{6+\delta}$ ($T_c \leq 128$ K), *Physica C*, 216, 29-35, (1993).
- [86] M.Marezio, P.Bordet, J.J.Capponi, P.P.Edwards, I.Gameson, W.I.F.David and A.R.Armstrong, "Crystal Structure of $Ba_2Ca_2Cu_3O_{8+\delta}$ at High Pressure (to

8.55 GPa) Determined by powder neutron Diffraction”, *Physical Review, Serie 3. B - Condensed Matter* (18,1978-), 52, 15551-15557, (1995).

[87] L.G.Johansson, P.Berastegui, Yu.Eeltsev, A.M.Grishin, I.Bryntse, A.Paszewin, T.Lada, A.Morawski, E.Olsson, and R.Gatt, “Hg-1212 and Hg-1223 Single Crystals: Synthesis and Characterisation” *Physica C*, 276, 270-276, (1997).

[88] J.L.Tholence, A.Santoro, S.N.Putilin, M.Marezio, S.M.Loureiro, O.Chmaissem, C.Chailout, J.J.Capponi and E.V.Antipov,”Synthesis and Neutron Powder Diffraction Study of The Superconductor $HgBa_2CaCu_2O_{6+\delta}$ Before and After Heat Treatment”, *Physica C*, 218, 348-355, (1993).

[89] G.J.Shen, X.X.Yao, Z.Y.Zheng, S.Y.Ding, X.Jin, X.N.Xu, and Y.Yu, “Anew Family of Cuprate With 1212 Structure: $SnBa_2CaCu_2O_Y$ ”, *Physica Status Solidi, Sectio A: Applied Research*, 163, 177 - 180, (1997).



جمهورية العراق
وزارة التعليم العالي والبحث العلمي
جامعة النهرين / كلية العلوم

تحضير المركبات الجديدة Sn-1223 و Cu-1223 الفائقة التوصيل العالي من Hg-1223

رسالة

مقدمة الى مجلس كلية العلوم / جامعة النهرين
وهي جزء من متطلبات نيل درجة الماجستير في الفيزياء

من قبل

أسراء ماهر جمال

بكالوريوس ٢٠١٤

بإشراف

د. عماد الشكرجي

ذو القعدة، ١٤٣٨ هـ

تموز، ٢٠١٧ م